A compact S^4 anomaly channel for the cosmological constant

Howard Lee
Independent Researcher, London, United Kingdom
howard@howardlee.me

August 2026

Abstract

The cosmological-constant problem is usually framed as a sum of absolute vacuum energies. On compact conformally flat S^4, however, the vacuum functional is degenerate with the cosmological counterterm. We prove that after finite local counterterms are quotiented out, the type-A Euler anomaly coefficient is the unique nonvanishing scheme-independent datum in the local linear constant-Weyl response. For the minimal Standard Model, $a_{\rm SM} = 1991/720 = 2.76528$. Its ordinary metric variation gives an H^4 stress and no small-curvature branch.

The compact channel is defined by a normalised matrix element between two equatorial cap states. This separates the fixed gravitational saddle from an external Weyl source. The round-S^4 action supplies $e^{-24\pi^2}$. Under the two-part matching hypothesis of endpoint conjugacy and reflection-even readout, the insertion lies on the unique fixed plane $h_*^2 = m_p M_{\rm P}$, and the one-cap curvature-charge response gives $h_*^2/M_{\rm P}^2 = m_p/M_{\rm P}$.

With the proposed four-form completion, and on the late-time branch where the regulated non-vacuum trace average vanishes, the compact charge becomes the residual cosmological curvature:

$$\frac{\Lambda_\infty}{M_{\rm P}^2} = q_{\rm WZ} = a_{\rm SM}\frac{m_p}{M_{\rm P}}e^{-24\pi^2} = 2.856 \times 10^{-122}.$$

The Planck 2018 flat-ΛCDM inference is $(2.846 \pm 0.057) \times 10^{-122}$; the central values differ by 0.4% (0.18σ). No parameter is fitted to the cosmological value. The completion also cancels constant shifts of the matter Lagrangian and predicts a spacetime-constant source with $w = -1$.

Keywords: cosmological constant, compact S^4, conformal anomaly, de Sitter saddle, semiclassical gravity, QCD dimensional transmutation, scale selection

1 Introduction

The discovery of late-time acceleration came from Type Ia supernovae [1, 2]. The observed dark-energy density, written as an equivalent cosmological-constant density $\rho_\Lambda/M_{\rm P}^4 = (\Lambda/M_{\rm P}^2)/(8\pi) \approx 1.1 \times 10^{-123}$, is smaller than the Planck density by roughly 120 orders of magnitude, and smaller than the electroweak scale to the fourth power by roughly 55 [3, 5, 6, 7, 8]. Standard treatments sum zero-point energies and ask why the total nearly cancels. Anthropic and landscape approaches [9, 10, 11] replace prediction with environmental selection across $\sim 10^{500}$ vacua. On compact Euclidean backgrounds, this question requires reformulation. The ambiguity is not created by compactness: even in flat space the absolute vacuum-energy density is not a scheme-independent observable. On round S^4 without boundary the situation is sharper still, because the vacuum-energy functional and the cosmological-counterterm functional are the *same* local operator $\int\sqrt{g}\,d^4x$ (Sec. 3). The conclusion that the zero-point sum simply renormalises the bare cosmological constant has been drawn explicitly by Bianchi and Rovelli [18] and by Hollands and Wald [19] in the semiclassical gravity context. Recent work has sharpened adjacent aspects of the same problem, including UV/IR constraints on QFT state counting, effective-gravity analyses involving the Standard Model, and global-constraint or unimodular reformulations [78, 79, 83]. Before one can ask whether the Standard Model predicts Λ, one must identify what compact-S^4 datum is actually protected against renormalisation ambiguity.

We first show that, among local linear constant-Weyl responses of the renormalised effective action satisfying counterterm invariance (C1) and conformal-flatness universality (C2), the type-A conformal anomaly coefficient is the unique nonvanishing scheme-independent compact matter datum on conformally flat S^4. This result requires no de Sitter contour choice and no scale selection; it is a theorem about the compact representative itself. Evaluated for the Standard Model, the extracted datum is $a_{\rm SM} = 1991/720 = 2.76528$.

Physical logic of the construction. The counterterm quotient leaves the Euler/Wess–Zumino coefficient as the protected compact matter datum. Because its local metric variation has the wrong H^4 scaling, the cosmological application also needs an infrared scale and an equation for the scalar curvature mode. QCD supplies the stable infrared endpoint, the selected round-S^4 saddle supplies the exponential weight, and a paired-cap Weyl response supplies the hierarchy factor. A separate four-form action maps the resulting dimensionless charge to residual curvature.

The compact calculation gives

$$q_{\rm WZ} = a_{\rm SM}\frac{m_p}{M_{\rm P}}e^{-24\pi^2},$$

while the global-source equation gives $\Lambda/M_{\rm P}^2 = q_{\rm WZ}$ on a maximally symmetric vacuum. On the late-time branch this identification additionally requires the regulated non-vacuum trace average to vanish. The same global-source equation predicts $w = -1$ wherever its residual constant is identified with dark energy. Together,

$$\boxed{\frac{\Lambda_\infty}{M_{\rm P}^2} = a_{\rm SM}\frac{m_p}{M_{\rm P}}e^{-24\pi^2} = 2.856\times10^{-122}}. \tag{1}$$

The Planck 2018 flat-ΛCDM-inferred value is $(2.846\pm0.057)\times10^{-122}$, a 0.4% central-value difference. The hierarchy separates into the 103 decades of compact-saddle suppression and the 19 decades of the QCD-to-Planck ratio, multiplied by the rational Standard Model Euler residue.

The compact charge is conditional on the suppressed compact thimble, the exact Planck boundary, the proton endpoint rule, and the two-part paired-cap matching hypothesis. Its cosmological interpretation additionally assumes the global-source action and, for the quoted late-time amplitude, the regulated trace-average condition. The on-saddle and modulus-integral readings are displayed separately in Sec. 14.2. None of these inputs is varied continuously against the observed value.

We use $\kappa^2 = 8\pi G$ and the unreduced Planck mass $M_{\rm P} = G^{-1/2} = 1.221\times10^{19}$ GeV [4]. The matched observable is $\Lambda/M_{\rm P}^2 = G\Lambda$; the compact saddle coordinate $u = \kappa^2\Lambda$ differs by a factor of 8π.

Relation to Padmanabhan's mode-count formula. Padmanabhan obtained

$$\Lambda L_P^2 = 3\exp(-24\pi^2\mu) \tag{2}$$

from a phase-space count of modes crossing the Hubble radius through an early inflationary era, radiation–matter domination and late acceleration [27, 28, 29]. In the 2012 construction the initial de Sitter radius is set to L_P, the Planck-domain Hubble-sphere count is taken to be $N = 4\pi$, and the order-one factor μ collects uncertainties in horizon crossing and the cosmic transitions. That construction also notes that ordinary continuum spin-2 perturbation theory would place Planck-scale inflation in conflict with primordial gravitational-wave bounds, and argues that the continuum calculation need not remain trustworthy at the Planck scale [27].

This shared numerical form does not constitute precedence for the present derivation. The calculational objects and physical decompositions are different. Padmanabhan's construction contains no compact-S^4 counterterm quotient, Euler/Wess–Zumino extraction, Standard Model anomaly census, proton endpoint, paired-cap readout or four-form completion. The present construction contains no Hubble-crossing mode count, cosmic-era matching, reheating prescription or Planck-scale inflationary history. Here $24\pi^2$ is the round-S^4 Einstein action at the declared Euclidean Planck boundary, while the additional nineteen decades arise as the multiplicative protected response $a_{\rm SM}m_p/M_{\rm P}$. The Planckian input is therefore a compact ultraviolet boundary, not a physical inflationary epoch, and it carries no associated prediction of Planck-scale primordial tensor fluctuations.

For numerical comparison only, with $L_P^2 = G = M_{\rm P}^{-2}$ the present result can be rewritten in Padmanabhan's form as

$$\mu_{\rm eff} = 1 + \frac{1}{24\pi^2}\ln\left(\frac{3M_{\rm P}}{a_{\rm SM}m_p}\right) = 1.18615. \tag{3}$$

This is an algebraic translation, not a determination of the μ defined by the mode-count construction and not independent corroboration of the present result. Because both formulas invoke Planckian de Sitter geometry, the common coefficient $24\pi^2$ is noted as a structural parallel rather than counted as a second derivation.

Relation to other approaches. Euclidean, QCD, thermodynamic and emergent-gravity approaches supply useful contrasts [22, 23, 24, 33, 25, 26, 30]. Here the compact de Sitter geometry computes a protected connected response; the QCD endpoint and Standard Model type-A residue close the hierarchy, while a separate four-form action maps that response to vacuum curvature.

The construction is closest on the gravity side to trace-free and vacuum-energy-sequestering approaches, which remove homogeneous vacuum shifts but generally leave a residual curvature as an integration constant, flux, or boundary datum [68, 40, 41, 42, 83]. Here the protected compact Wess–Zumino response supplies a candidate value for that residual. The compact extraction, strict-channel response, and global curvature map are logically distinct.

Framework and scope. We work at leading saddle order in the sourced compact de Sitter functional (see also recent QFT-in-curved-spacetime and semiclassical- gravity scope discussions [84, 93]). Classical metric saddles enter through their Einstein–Hilbert action, and Standard Model matter is quantised on the selected saddle. The protected coefficient is the matter-QFT Euler anomaly rather than a graviton anomaly census. Source-independent metric and ghost determinants cancel in the sector-normalised cap response; source-dependent gravitational dressing and higher-curvature changes to the primitive action remain outside the leading matter-QFT truncation. The compact response and the gravity-side completion remain logically separate. Table 1 summarises their status.

Conventions. We work in Euclidean signature on round S^4 throughout, with Ricci tensor $R_{\mu\nu} = \Lambda g_{\mu\nu}$ (positive scalar curvature $R = 4\Lambda > 0$) and Riemann sign such that the Euler density is $E_4 = R_{\mu\nu\rho\sigma}R^{\mu\nu\rho\sigma} - 4R_{\mu\nu}R^{\mu\nu} + R^2$, with $\int_{S^4}\sqrt{g}\,E_4 = 32\pi^2\chi(S^4) = 64\pi^2$. The trace anomaly [73] is normalised as in [20, 21], $\langle T^\mu{}_\mu\rangle = (c/16\pi^2)W^2 - (a/16\pi^2)E_4 + \text{tot. deriv.}$, and the Euclidean Einstein–Hilbert action is $S_{\rm EH} = -(1/2\kappa^2)\int(R - 2\Lambda)\sqrt{g}\,d^4x$. We use H for the dimensionful curvature label of the S^4 modulus, defined so that the on-shell Einstein–Hilbert action takes the canonical form $|S_{\mathrm{EH}}| = 24\pi^2 M_{\mathrm{P}}^2/H^2$; equivalently $H^2 = 8\pi\Lambda$. This H is distinct from the Lorentzian de Sitter expansion rate $H_{\mathrm{dS}}^2 = \Lambda/3$ (the two differ by a factor of 24π) and from the observed Hubble constant H_0. We denote the fixed gravitational-sector label by u_s and the external compensator scale in its normalised matter cap by h. They are distinct arguments of the paired-cap amplitude; under the two-part matching hypothesis, the insertion lies on the fixed plane $h_*^2 = m_p M_{\mathrm{P}}$.

2 Overview of the construction

The central construction separates the gravitational sector from the matter source. Let g_s be a fixed round-S^4 saddle labelled by u_s, and cut it at the equator $\Sigma = S^3$. A constant external Weyl source acts on one cap through

$$\widehat{g}_{\mu\nu}(h) = x_h g_{s,\mu\nu}, \qquad x_h \equiv \frac{M_{\mathrm{P}}^2}{h^2}.$$

The sourced cap prepares a state in $\mathcal{H}_{\Sigma,x_h\gamma_s}$. The compensator-induced Weyl transport U_h : $\mathcal{H}_{\Sigma,x_h\gamma_s} \to \mathcal{H}_{\Sigma,\gamma_s}$ places it in the fixed fiducial boundary Hilbert space. After removing the common classical sphere grade, the reduced paired-cap amplitude is

$$Z_{n,+}(h\,|\,u_s) \equiv \langle \Omega_{n,-}(u_s)|U_h|\Psi_{n,+}^{(h)}(u_s)\rangle_{\Sigma,\gamma_s}, \qquad \mathcal{Z}_{n,+}^{\mathrm{full}} = e^{-nB(u_s)} Z_{n,+}. \tag{4}$$

The anomalous Jacobian of the Weyl transport is included in $Z_{n,+}$. The normalised cap action is

$$\Delta\Gamma_{n,+}(h\,|\,u_s) \equiv -\ln \frac{Z_{n,+}(h\,|\,u_s)}{Z_{n,+}(M_{\mathrm{P}}\,|\,u_s)}, \qquad \Delta\Gamma_{n,+}(M_{\mathrm{P}}\,|\,u_s) = 0. \tag{5}$$

The same bra appears in numerator and denominator, so its overall normalisation and phase cancel. Its boundary functional remains part of the matrix element. The two arguments now have distinct roles: u_s labels the gravitational saddle, while h labels an external trace source on that saddle. Because the classical grade has been removed from $Z_{n,+}$, the explicit factor e^{-B_s} below is counted once.

The additive one-cap Einstein curvature charge provides the source coordinate,

$$\mathcal{C}_+(h) \equiv \frac{1}{4\kappa^2}\int_{D_+^4} d^4x \sqrt{\widehat{g}(h)}\, R[\widehat{g}(h)] = 12\pi^2 x_h, \quad \mathcal{C}_{+,0} = \mathcal{C}_+(M_{\mathrm{P}}) = 12\pi^2, \quad \mathcal{D}_+ \equiv \mathcal{C}_{+,0}\frac{d}{d\mathcal{C}_+(h)}.$$

For the primitive sector at $u_s = 1$, the compact charge is

$$q_{\mathrm{WZ}} \equiv e^{-24\pi^2}\, \mathcal{D}_+\Delta\Gamma_{1,+}(h\,|\,1)|_{h=h_*} + O(e^{-48\pi^2}). \tag{6}$$

The extraction theorem gives the universal one-cap Euler response $\Delta\Gamma_{A,+} = \mathcal{A}_m(h)\ln x_h$, hence

$$\mathcal{D}_+\Delta\Gamma_{A,+}(h) = \mathcal{A}_m(h)\frac{h^2}{M_{\mathrm{P}}^2}.$$

The Standard Model fixes $\mathcal{A}_m(h_*) = a_{\mathrm{SM}} = 1991/720$ at leading order. The infrared endpoint is the stable proton pole. Under the two-part matching hypothesis of endpoint conjugacy and reflection-even readout, the insertion lies on the unique fixed plane

$$h_*^2 = m_p M_{\mathrm{P}}.$$

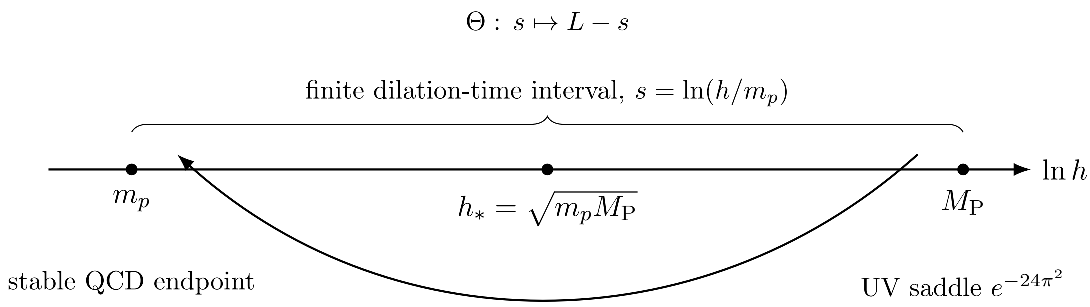

Figure 1: The finite logarithmic interval between the stable QCD and Planck endpoint standards. Under the two-part matching hypothesis of endpoint conjugacy and reflection-even readout, the insertion lies on the fixed plane $h_*^2 = m_p M_{\mathrm{P}}$. The primitive gravitational sector supplies the separate weight $e^{-24\pi^2}$.

Table 1: Logical structure of the result. Derived consequences are separated from physical inputs.

Layer	Status	Location
Compact matter datum	type-A extraction theorem; $a_{\mathrm{SM}} = 1991/720$	Secs. 3–5
Local gravity	H^4 obstruction and unique trace-free projection	Sec. 7
Compact sector	suppressed round-S^4 thimble at the exact boundary $u_b = 1$	Sec. 9
Paired-cap response	scalar matrix element in a fixed boundary Hilbert space and one-cap curvature-charge derivative; matching assumes endpoint conjugacy and a reflection-even readout	Secs. 10–11
Infrared endpoint	stable proton trace-charge standard under the stated endpoint rule	Sec. 8
Global completion	four-form action is proposed; its field equations and $w = -1$ consequence are derived	Sec. 12
Late-time amplitude	$\Lambda_\infty/M_{\mathrm{P}}^2 = q_{\mathrm{WZ}}$ requires the regulated non-vacuum trace average to vanish	Sec. 13

Substitution into Eq. (6) gives

$$q_{\mathrm{WZ}} = a_{\mathrm{SM}} \frac{m_p}{M_{\mathrm{P}}} e^{-24\pi^2} = 2.856 \times 10^{-122}. \tag{7}$$

The four-form completion is logically separate. It gives $\Lambda/M_{\mathrm{P}}^2 = q_{\mathrm{WZ}}$ on a maximally symmetric vacuum and a constant residual source with $w = -1$. The late-time amplitude additionally requires the regulated non-vacuum trace average to vanish:

$$\frac{\Lambda_\infty}{M_{\mathrm{P}}^2} = q_{\mathrm{WZ}}. \tag{8}$$

3 The compact-S^4 vacuum-energy ambiguity

The cosmological counterterm $\alpha \int \sqrt{g}$ in the renormalised effective action of any QFT on a curved background is a familiar feature of semiclassical gravity [12, 16, 17, 7]. In flat space, the absolute vacuum-energy density is not a scheme-independent observable: a hard cutoff gives the familiar quartic dependence on the cutoff, while dimensional regularisation gives a different mass-dependent contribution. What flat space does provide is a reference structure in which subtraction conventions can be imposed, and in which *differences* between configurations (Casimir-type energies) can be physically meaningful. On compact S^4 without boundary the situation is structurally sharper. There is a single compact configuration, and the vacuum-energy functional and the cosmological-counterterm functional are both scheme-dependent and the *same* local operator on S^4. Both reduce to $\int \sqrt{g}\, d^4x \propto H^{-4}$, with no geometrically distinguishable label separating them; no renormalisation condition intrinsic to the compact background splits the two. The observation that the standard zero-point sum simply renormalises the bare cosmological constant, and that the split between "vacuum energy" and "counterterm" is not a scheme-independent observable, has been made by Bianchi and Rovelli [18] and by Hollands and Wald [19]; related recent discussions also separate observable QFT effects from a literal absolute vacuum-energy fluid [80]. The absolute vacuum energy on S^4 is therefore not a scheme-independent observable. Any well-posed extraction must identify a counterterm-invariant functional.

The Casimir objection. A standard objection is that the Casimir effect demonstrates that vacuum energy is real and gravitates. The Casimir effect, however, measures the energy *difference* between two configurations on the same background, for example parallel conducting plates at separation d versus $d \to \infty$ [31]. This difference is scheme-independent because the cosmological counterterm contributes equally to both configurations and cancels in the subtraction. On compact S^4 without boundary there is no second configuration: the partition function is a single number, the counterterm ambiguity does not cancel, and the result is scheme-dependent. (Indeed, Jaffe [32] has shown that Casimir forces can be derived entirely from relativistic van der Waals interactions, without reference to zero-point vacuum fluctuations.) Scheme-independent vacuum-energy *differences* between phases, such as the QCD condensation energy $\Delta V \sim \Lambda_{\mathrm{QCD}}^4 \sim 10^{-4}\,\mathrm{GeV}^4$ between confined and deconfined phases, are physical. The completed global equation cancels a strictly homogeneous constant shift but does not erase spacetime-dependent phase-transition dynamics, interfaces, or other inhomogeneous stresses; those remain a separate cosmological-history problem.

Three direct identifications one might try for Λ from the compact path integral on the de Sitter saddle all produce wrong answers:

(i) *Free energy per four-volume*, $\Lambda = -T \ln Z / V_3$. The zero-mode integral absorbs the hierarchy into an $O(1)$ partition function; the Gibbons–Hawking temperature and three-volume restore Planck-scale vacuum energy regardless of H.

(ii) *Full effective action at the evaluation scale*, $\Lambda \sim \Gamma(h_*)$. The classical piece $S_{\mathrm{cl}} = 24\pi^2 M_{\mathrm{P}}/m_p \approx 3 \times 10^{21}$ gives absurd over-suppression (confusing the matching scale with the Planck curvature of the saddle).

(iii) *Partition function itself*, $\Lambda \propto Z$. The matter determinant gives $Z_{\mathrm{matter}} \propto (H/\mu)^{4a_{\mathrm{SM}}}$, with a_{SM} in the exponent. No thermodynamic operation converts $(\mathrm{const})^{a_{\mathrm{SM}}}$ into a_{SM}.

All three failures share a common root: they attempt to extract Λ directly from Z or Γ, which are contaminated by scheme- and measure-dependent contributions. The underlying degeneracy, namely that the vacuum-energy term and cosmological counterterm multiply the same operator, leaves no physical energy difference to extract. A *well-posed* extraction must be invariant under every allowed renormalisation ambiguity. A quantitative classification of the inequivalent readings of the compact channel itself, including the bounded-window modulus integral, is given in Sec. 14.2.

4 Extraction theorem on conformally flat S^4

$\Gamma[g]$ is defined only up to local counterterms. We therefore specify minimal consistency requirements for any extraction of a physical Λ from the compact path integral on S^4.

Local counterterm ambiguities. For any QFT on a curved background, renormalisation permits adding local curvature counterterms to $\Gamma[g]$:

$$\begin{aligned}\Gamma[g] \;\rightarrow\; \Gamma[g] &+ \alpha\int d^4x\sqrt{g} + \beta\int d^4x\sqrt{g}\,R \\ &+ \gamma\int d^4x\sqrt{g}\,R^2 + \delta\int d^4x\sqrt{g}\,W^2 + \epsilon\int d^4x\sqrt{g}\,E_4 + \cdots\,,\end{aligned} \tag{9}$$

together with scheme-dependent total derivatives such as $\int\sqrt{g}\,\Box R$. This is the complete dimension-four local curvature basis (modulo the Lanczos identity expressing $\int\sqrt{g}\,R_{\mu\nu}R^{\mu\nu}$ as a linear combination of the above). The $\alpha\int\sqrt{g}$ term is the cosmological counterterm; shifting the matter Lagrangian by a constant $\mathcal{L}_m \to \mathcal{L}_m + \rho_0$ is equivalent to $\alpha \to \alpha + \rho_0$. Any putative extraction of a physical Λ from Z must be insensitive to these shifts; otherwise $Z \to \Lambda$ is not a prediction of the compact path integral but an artefact of the regularisation.

Extraction criteria. We require the extraction functional $\mathcal{F}[\Gamma; S^4(H)]$ to satisfy:

C1 (Counterterm/scheme invariance): $\mathcal{F}$ is invariant under all local counterterm ambiguities of Eq. (9), including $\alpha\int\sqrt{g}$ (cosmological counterterm), $\beta\int\sqrt{g}\,R$, higher-curvature terms, and total-derivative ambiguities, so that $\mathcal{F}$ constitutes a well-posed prediction of the path integral.

C2 (Conformally-flat universality): on round S^4 ($W^2 = 0$), the extracted quantity depends only on diffeomorphism-invariant, scheme-independent universal data of the matter sector, not on gauge-volume normalisations, measure conventions, or regulator artefacts.

Theorem 1 (Euler extraction on conformally flat S^4)**.** *On round conformally flat $S^4(H)$, among local linear constant-Weyl responses of the renormalised effective action satisfying counterterm invariance (C1) and conformal-flatness universality (C2), the unique nonvanishing H-independent scheme-independent matter datum is the type-A Euler anomaly coefficient. With $\Gamma(H) = -\ln Z[S^4(H)]$ and*

$$\langle T_{\mu\nu}\rangle = \frac{2}{\sqrt{g}}\frac{\delta\Gamma}{\delta g^{\mu\nu}},$$

it is isolated at a conformal fixed point by

$$\mathcal{A}[\Gamma] = -\frac{1}{4}\Pi_{H^0}\left(\frac{d\Gamma(H)}{d\ln H}\right). \tag{10}$$

Here Π_{H^0} extracts the coefficient of the H^0 term in the local constant-Weyl response after beta-function and operator-mixing contributions have been separated. Away from a fixed point, the same statement applies to the Euler-cocycle projection of the local RG equation after beta-function and operator-mixing terms have been separated [37].

Proof. The local counterterms in Eq. (9) evaluate on $S^4(H)$ as H^{-4}, H^{-2}, a constant, zero, a topological constant, and zero for the volume, Einstein, R^2, W^2, E_4, and $\Box R$ terms, respectively. After $d/d\ln H$, they are therefore either H-dependent or vanish. A finite E_4 counterterm changes only the constant part of Γ and cannot absorb the anomalous logarithm.

The sign is fixed by the Euclidean variational convention. Under a constant Weyl variation $g_{\mu\nu} \to e^{2\sigma} g_{\mu\nu}$, $\delta g^{\mu\nu} = -2\sigma g^{\mu\nu}$, so

$$\begin{aligned} \delta_\sigma \Gamma[g] &= -\int d^4x \sqrt{g}\, \sigma \langle T^\mu{}_\mu \rangle \\ &= +\frac{a}{(4\pi)^2} \int d^4x \sqrt{g}\, \sigma E_4 \end{aligned} \tag{11}$$

for the anomaly convention of Eq. (12). On conformally flat S^4, $W^2 = 0$, the integrated total derivative vanishes, and $\int_{S^4} \sqrt{g}\, E_4 = 64\pi^2$. Hence $\delta_\sigma \Gamma = 4a\sigma$. Since a Weyl enlargement of the sphere sends $H \to e^{-\sigma} H$, one has $\sigma = -\delta \ln H$, and therefore

$$\Pi_{H^0}\left(\frac{d\Gamma}{d \ln H} \right) = -4a.$$

Equation (10) follows. Wess–Zumino consistency protects the coefficient [36]. At a fixed point the argument is loop-order independent: a local curvature term of order n scales as H^{2n-4}, while the only undressed logarithmic response in the conformally flat local cohomology is the Euler cocycle. For a running theory the local-RG Euler projector removes the additional $\beta^i \partial\Gamma/\partial g^i$ and operator-mixing responses. □

Free-scalar sign audit. For one real conformally coupled scalar, $a_s = 1/360$ and the conformal Laplacian on S^4 has $\zeta_{\Delta_c}(0) = -1/90$. Because its eigenvalues scale as H^2,

$$\Gamma_s = \frac{1}{2} \ln \det(\Delta_c/\mu^2) = \frac{1}{90} \ln \frac{\mu}{H} + \text{constant}, \qquad \frac{d\Gamma_s}{d \ln H} = -\frac{1}{90} = -4a_s.$$

This determinant check fixes the sign independently of the Ward-identity argument and agrees with the standard even-dimensional sphere-free-energy convention [94].

Standard Model corollary. In the effectively massless Standard Model window, the protected matter response is $\mathcal{A}_m(H) = a_{\rm SM} + O(m_i^2/H^2)$, with $a_{\rm SM} = 1991/720$ at leading free-field order. Interaction and broader determinant corrections are treated separately in Sec. 13.

Scope of the theorem. The theorem fixes the one-dimensional protected matter direction entering the connected compact response: it is the Euler coefficient a. It does not state that an ordinary metric variation of this datum produces the Friedmann cosmological constant; Sec. 7 shows that the corresponding local stress scales as H^4. The gravity-side map is therefore a separate ingredient.

Relation to the standard trace anomaly. The trace anomaly and Gauss–Bonnet integral are standard. The added content here is the counterterm-by-counterterm classification on compact round S^4: every allowed local ambiguity has either an H-dependent response or zero response under $d/d \ln H$, leaving the anomalous logarithm as the unique nonzero constant term.

Interpretation of the extracted datum. The protected coefficient $a_{\rm SM}$ corresponds to a protected *object*: on $S^4(H)$, the matter effective action contains the anomaly-induced logarithm $+4a_{\rm SM} \ln(\mu/H)$, the unique part whose response to a constant Weyl rescaling produces the H-independent constant $-4a_{\rm SM}$. This logarithm is the round-S^4 reduction of a non-local Wess–Zumino representative of the four-dimensional trace anomaly [43, 44, 71, 82, 38]. The extraction map in Eq. (10) projects onto its Euler coefficient. The remaining effective action may contain local counterterm classes, beta-function/operator responses, and a Weyl-invariant complement; the projector excludes these additional structures without asserting that they vanish.

Table 2: The a-anomaly coefficient per field.

Field type	a
Real scalar	1/360
Weyl fermion	11/720
Vector boson	31/180

5 Standard Model evaluation of the extracted datum

In four dimensions, the trace of the stress-energy tensor of a quantum field on a curved background contains two central charges [20, 21]:

$$\begin{aligned}\langle T^{\mu}{}_{\mu}\rangle \;=\; &\frac{c}{16\pi^2}\,W_{\mu\nu\rho\sigma}W^{\mu\nu\rho\sigma} \;-\; \frac{a}{16\pi^2}\,E_4\\ &+\;(\text{total derivatives})\,,\end{aligned} \tag{12}$$

where $W_{\mu\nu\rho\sigma}$ is the Weyl tensor and $E_4 = R^2 - 4R_{\mu\nu}R^{\mu\nu} + R_{\mu\nu\rho\sigma}R^{\mu\nu\rho\sigma}$ is the Euler density. At a free-field conformal fixed point, the coefficients a and c are dimensionless numbers fixed by the field content; in an interacting theory their fixed-point values can receive interaction-dependent corrections.

On the round S^4, which is conformally flat ($W_{\mu\nu\rho\sigma} = 0$), the c-anomaly drops out entirely. Of the two central-charge terms, only the a-anomaly contributes to the universal constant-Weyl response on round S^4. At conformal fixed points, a is the quantity constrained by the four-dimensional a-theorem [74, 45]. On S^4 it couples to the Euler density E_4, the same topological structure appearing in the gravitational action via Eq. (24).

The standard a-coefficients per free field [13, 14, 46, 47] are listed in Table 2; recent path-integral analyses of Weyl-fermion trace anomalies provide a modern check on the fermionic sector [85].
The Standard Model contains 4 real scalars (Higgs doublet), 45 Weyl fermions (3 generations $\times$ 15 per generation), and 12 vector bosons (8 gluons $+W^{\pm} + Z + \gamma$) [4]. Therefore:

$$a_{\rm SM} \;=\; \frac{4}{360} + \frac{45\times 11}{720} + \frac{12\times 31}{180} \;=\; \frac{1991}{720} \;=\; 2.76528\,. \tag{13}$$

This is a rational number fixed by the known particle content. In the effectively massless regime ($m_i/H \ll 1$) relevant here, the Euler (type-A) anomaly is fixed by field content up to controlled interaction and mass corrections; we use the standard free-field value and treat residual corrections in the error budget (Sec. 13). At the evaluation scale $h_* = \sqrt{m_p\,M_{\rm P}} \approx 3.4\times 10^9$ GeV, all Standard Model species satisfy $m_i/h_* \ll 1$; the largest correction is $(m_{\rm top}/h_*)^2 \approx 3\times 10^{-15}$ [4]. The Standard Model is not exactly conformal. The free-field fixed-point Euler coefficient is universal and scheme-independent; at the running evaluation scale the relevant $a_{\rm eff}(h_*)$ is defined by the local-RG Euler-cocycle projection, with beta-function, operator mixing, interaction and mass effects kept separate and budgeted in Sec. 13. In particular, the scalar field-count value 1/360 is independent of the Higgs nonminimal curvature coupling $\xi\,|H|^2R$. Away from conformal coupling, the full scalar trace may contain additional nonconformal local structures, including an R^2 term as well as the scheme-dependent total derivative $\Box R$; nevertheless the type-A Euler and type-B Weyl coefficients themselves are independent of ξ [13, 12, 15]. On round S^4, $\int\sqrt{g}\,R^2$ is independent of H and is annihilated by $d/d\ln H$, while $\int\sqrt{g}\,\Box R = 0$ by compactness. The extracted Euler datum $a_{\rm SM} = 1991/720$ is therefore ξ-independent, and no assumption $\xi = \frac{1}{6}$ is required. The leading simple non-CFT estimate is $O(y_t^2/16\pi^2) \approx 0.2\%$. In the absence of a complete curved-space Standard Model cap calculation, we use $\lesssim 0.5\%$ as a provisional matter-response estimate rather than a calculated uncertainty (Sec. 13). It is below the separate $\sim 4\%$ endpoint-relaxation robustness envelope.

Inverting Eq. (1), the anomaly coefficient *inferred* from observation is

$$\boxed{a_{\rm inf} \;\equiv\; \frac{(\Lambda/M_{\rm P}^2)_{\rm obs}}{(m_p/M_{\rm P})\, e^{-24\pi^2}} \;=\; 2.755 \pm 0.055\,,} \tag{14}$$

where the displayed uncertainty is the observational uncertainty from Planck 2018 [3] with the zero-temperature proton endpoint held fixed. If the endpoint criterion is relaxed to include the nearby thermal diagnostic $2\pi T_c$ [55], the interpretive robustness envelope broadens to $\sim 4\%$; that broader envelope is not included in the displayed error bar for $a_{\rm inf}$. Equivalently, $a_{\rm inf}/a_{\rm SM} = 0.996$, a 0.4% difference, so the inferred compact residue agrees with the Standard Model value within the displayed observational uncertainty.

Within the leading Einstein–Hilbert paired-cap channel, a confirmed weakly coupled field-content shift exceeding the $\sim 4\%$ endpoint-relaxation envelope would produce a visible mismatch. It becomes a falsifier once source-dependent gravitational dressing and the higher-curvature correction to the primitive action are controlled below that level. With the selected zero-temperature proton endpoint, the observational comparison is the narrower $\pm 2.0\%$, supplemented by the estimated $\lesssim 0.5\%$ matter-channel correction envelope. Future collider discoveries therefore provide conditional changes to the compact residue, not automatic cosmological exclusions.

Local-RG analyses distinguish the physical Euler coefficient from beta-function-proportional flow terms in the $\widetilde{A}$-function [37, 50]. Jack and Poole construct the gauge-theory a-function through four-loop order and provide nontrivial consistency relations, but this is not by itself a curved-space Standard Model calculation. In the explicit locally covariant ϕ^4 analysis of Fröb and Zahn, the E_4 coefficient is fixed and its interaction correction vanishes through second order; their discussion also records the known higher-order onset $O(\lambda^4)$ for the scalar a coefficient [67]. These results support the absence of a generic leading $O(g^2)$ shift in the examples controlled so far, but do not supply a complete Standard Model number at h_*. We therefore use the rational free-field value as the leading term and retain a conservative $\lesssim 0.5\%$ matter-response envelope. By itself this order-unity number cannot explain 122 decades of hierarchy; a genuinely infrared input is needed.

6 Need for a separate infrared input in direct compact-saddle mechanisms

Before assembling the formula, we show that none of the direct mechanisms available in the stated single-saddle treatment produces the linear factor $m_p/M_{\rm P} \approx 10^{-19}$. The three arguments below cover direct zero-mode sampling, local heat-kernel mass corrections, and Planck-scale QCD instantons. They motivate a separate infrared input within this treatment; they are not asserted as a no-go theorem for every possible nonlocal or UV-complete compact effect.

(i) Zero-mode localisation. Within the declared sub-Planckian domain $x = M_{\rm P}^2/H^2 \geq 1$, the classical weight is exponentially localised at the boundary $x = 1$. The confinement region $H \sim m_p$ lies ~ 44 e-foldings away in $\ln H$ and carries an additional action of order $24\pi^2 M_{\rm P}^2/m_p^2 \sim 10^{40}$. The direct modulus integral therefore never samples the confinement scale. The fractional boundary-layer width $1/B$ belongs to the bounded R2 reading, not to the R3 response prescription.

(ii) Local analytic mass expansion. In the local analytic part of the one-loop heat-kernel expansion on a compact Riemannian manifold, mass dependence enters through m^2, giving powers $(m\,a)^{2n}$ (with logarithms multiplying even powers) rather than a term linear in $m\,a$ [51]. For $m\,a = m_p/M_{\rm P}$, the first such correction is of order 10^{-38}.

(iii) QCD instanton suppression. A perturbative Standard Model RG extrapolation gives $\alpha_s(M_{\rm P}) \approx 0.02$ [69]. The corresponding Yang–Mills instanton action is $S_{\rm QCD} = 2\pi/\alpha_s \approx 314$ [65]; the amplitude $e^{-314} \approx 10^{-136}$ is negligible compared with the required 10^{-19}.

Origin of the product form. The compact-channel expression has three factors with different origins. The extraction theorem fixes the matter input: after finite local counterterms have been quotiented out on conformally flat compact S^4, the only nonvanishing scheme-independent local matter residue in the constant-Weyl response is the Euler/Wess–Zumino coefficient a. For the minimal Standard Model this gives $a_{\rm SM} = 1991/720$. The Planck-curvature compact de Sitter thimble supplies the nonperturbative grade $e^{-24\pi^2}$. A finite external compensator in the normalised cap functional supplies the separate matter response, and the two-part matching hypothesis places its readout on the fixed plane $h_*^2 = m_p M_{\rm P}$, giving $h_*^2/M_{\rm P}^2 = m_p/M_{\rm P}$. The exclusion arguments above show why this infrared factor cannot be generated by a purely Planck-scale modulus integral; the QCD endpoint supplies the required physical infrared standard. Within the compact-channel prescription these ingredients give the connected response

$$q_{\rm WZ} = a_{\rm SM}\,\frac{m_p}{M_{\rm P}}\,e^{-24\pi^2}. \tag{15}$$

The extraction theorem fixes the compact matter residue. The paired-cap construction then defines its sector-resolved response, including the source sign, action normalisation and reflection point. The separate global-source action maps that compact charge to vacuum curvature, and Eq. (46) supplies the late-time amplitude condition.

7 Ordinary-GR obstruction and the trace-free quotient

The ordinary-GR obstruction. Let Λ_g denote the geometric cosmological constant of a round four-dimensional de Sitter solution. Then

$$R_{\mu\nu} = \Lambda_g g_{\mu\nu}, \qquad R = 4\Lambda_g, \qquad E_4 = \frac{8}{3}\Lambda_g^2.$$

With the anomaly convention $\langle T^\mu{}_\mu\rangle_A = -aE_4/(16\pi^2)$, maximal symmetry fixes

$$T^A_{\mu\nu} = -\frac{a\Lambda_g^2}{24\pi^2}g_{\mu\nu}.$$

Proposition 2 (Ordinary-GR no-go for a linear compact source)**.** *In ordinary semiclassical Einstein gravity the local type-A anomaly changes the round de Sitter curvature at order $\Lambda_g^2/M_{\rm P}^2$. Multiplying the anomaly sector by a small compact weight does not create a small branch linear in that weight.*

Proof. With a renormalised local cosmological term Λ_0,

$$G_{\mu\nu} + \Lambda_0 g_{\mu\nu} = \frac{8\pi}{M_{\rm P}^2}T^A_{\mu\nu}.$$

Since $G_{\mu\nu} = -\Lambda_g g_{\mu\nu}$ on the round branch,

$$\Lambda_g - \Lambda_0 = \frac{a}{3\pi}\frac{\Lambda_g^2}{M_{\mathrm{P}}^2}. \tag{16}$$

For $\Lambda_0 = 0$, the nonzero root is $\Lambda_g/M_{\mathrm{P}}^2 = 3\pi/a$, which is Planckian. If the anomaly sector is multiplied by a small coefficient ε, the nonzero root becomes $3\pi/(a\varepsilon)$: the suppression appears in the denominator. Thus no ordinary local metric variation yields $\Lambda_g/M_{\mathrm{P}}^2 \propto \varepsilon a$. □

The obstruction is structural. A protected dimensionless datum q could multiply a local volume term $qM_{\mathrm{P}}^4 \int \sqrt{|g|}$, but that is precisely the operator removed by the cosmological-counterterm quotient. A two-derivative term $qM_{\mathrm{P}}^2 \int \sqrt{|g|}R$ only renormalises Newton's constant, while curvature-squared terms produce qH^4 stresses. A linear protected relation therefore requires a global zero-mode equation.

The local equation on the volume-counterterm quotient. Write the two-derivative renormalised metric equation, before selecting a cosmological representative, as

$$\mathcal{E}_{\mu\nu} \equiv G_{\mu\nu} - \frac{8\pi}{M_{\mathrm{P}}^2}T_{\mu\nu}.$$

Adding a finite local volume term shifts $\mathcal{E}_{\mu\nu} \mapsto \mathcal{E}_{\mu\nu} + cg_{\mu\nu}$.

Lemma 3 (Trace-free quotient projector)**.** *The unique algebraic local projection of the metric equation that is independent of the representative $\mathcal{E}_{\mu\nu} \sim \mathcal{E}_{\mu\nu} + cg_{\mu\nu}$ is*

$$R_{\mu\nu} - \frac{1}{4}Rg_{\mu\nu} = \frac{8\pi}{M_{\mathrm{P}}^2}\left(T_{\mu\nu} - \frac{1}{4}Tg_{\mu\nu}\right). \tag{17}$$

For conserved matter stress, any solution of this projected equation leaves one spacetime constant Λ_{int} through

$$R + \frac{8\pi}{M_{\mathrm{P}}^2}T = 4\Lambda_{\mathrm{int}}. \tag{18}$$

Proof. The unique algebraic projection of a symmetric tensor that is invariant under $X_{\mu\nu} \mapsto X_{\mu\nu} + cg_{\mu\nu}$ and acts as the identity on traceless tensors is $X_{\mu\nu} - Xg_{\mu\nu}/4$. Applying it to $\mathcal{E}_{\mu\nu} = 0$ gives Eq. (17). The contracted Bianchi identity and $\nabla^\mu T_{\mu\nu} = 0$ then imply $\nabla_\nu(R + 8\pi T/M_{\mathrm{P}}^2) = 0$, giving Eq. (18). □

Renormalisation ambiguity alone does not select the physical dynamics. Lemma 3 identifies only the local equation that a source law compatible with the volume-counterterm quotient must reproduce. The compact global-source action of Sec. 12 is the sole gravity-side postulate. Its variation yields both Eq. (17) and the equation fixing the omitted scalar mode.

8 The infrared input from QCD: m_p/M_{P}

The proton mass arises from QCD confinement via dimensional transmutation [53, 54]:

$$m_p \approx \Lambda_{\mathrm{QCD}} \sim M_{\mathrm{UV}} \exp\left(-\frac{8\pi^2}{b_0\, g^2(M_{\mathrm{UV}})}\right), \tag{19}$$

where $b_0 = 7$ for SU(3) with six flavours. The ratio

$$\frac{m_p}{M_{\rm P}} \approx 7.685 \times 10^{-20} \tag{20}$$

Using the current proton and Planck masses [4], this ratio accounts for the remaining ~ 19 orders of magnitude. A perturbative coupling $\alpha_s(M_{\rm P}) \simeq 0.02 \simeq 1/50$ in the one-loop estimate exponentiates into a hierarchy of approximately nineteen decades. This mechanism has been understood since the 1970s and is not a cancellation; the proton mass is a non-perturbatively generated scale. The proton mass enters not because the vacuum contains protons, but because its pole is the stable, gauge-invariant, late-time representative of the QCD dimensional-transmutation endpoint in the full Standard Model. The mass is predominantly dynamical: lattice calculations attribute about 70% of it to quark and gluon field energies, while over 90% arises from QCD dynamics rather than Higgs-generated quark masses; the renormalisation-group-invariant QCD trace anomaly contributes $\approx 23\%$ [57, 58]. Recent lattice form-factor, NNLO, and first-principles energy–momentum-tensor studies develop these decompositions further and emphasise their renormalisation-scheme and scale dependence [88, 90, 91]. The endpoint is therefore taken to be the physical proton pole, not any individual decomposition term.

The 122-decade hierarchy thus decomposes as $103 + 19$: a de Sitter saddle suppression times a gauge hierarchy, with no cancellation. Using the physical ratio in Eq. (20), the compact response can be written as a single exponential suppression,

$$q_{\rm WZ} \ = \ a_{\rm SM} \ \exp\bigl[-(S_{\rm grav} + S_{\rm trans})\bigr], \qquad \frac{\Lambda}{M_{\rm P}^2} = q_{\rm WZ} \quad \text{under Eq. (42)}, \tag{21}$$

where $S_{\rm grav} = 24\pi^2 \approx 237$ and $S_{\rm trans} \equiv \ln(M_{\rm P}/m_p) = 44.01$. At one loop, dimensional transmutation gives $S_{\rm trans} \simeq 2\pi/[b_0\alpha_s(M_{\rm P})]$, up to threshold and order-one matching factors, with $\alpha_s \equiv g^2/4\pi$; the total exponent is approximately 281. The gravitational and confinement suppressions therefore add in the exponent. A formal derivation of their joint contribution is given through the sourced one-saddle construction in Sec. 11.

9 The compact de Sitter saddle weight $e^{-24\pi^2}$

The compact S^4 extraction theorem identifies the protected matter datum. The sourced semiclassical gravitational framework supplies the corresponding compact de Sitter saddle channel. This section fixes the saddle weight appearing in that channel and separates geometric facts from the contour prescription used to define the sourced cosmological operator.

Saddle geometry. The Einstein–Hilbert action evaluated on the round S^4 is

$$S_{\rm EH} = -\frac{1}{2\kappa^2}\int_{S^4} (R - 2\Lambda)\sqrt{g}\, d^4x = -\frac{24\pi^2}{\kappa^2\Lambda}\,. \tag{22}$$

The number $24\pi^2$ is the dimensionless Einstein–Hilbert action at the κ-Planck curvature point, not a count of unreduced Planck four-volumes. Introduce the instanton curvature variable

$$u \equiv \kappa^2\Lambda$$

so that

$$|S_{\rm EH}| = \frac{24\pi^2}{u}\,.$$

The compact S^4 saddle here is the ultraviolet gravitational sector of the sourced trans-series, not the observed late-time de Sitter solution. The semiclassical saddle weight is normalised at the Planck-curvature endpoint $u = \kappa^2\Lambda = 1$ set by Newton's constant, and

$$|S_{\mathrm{EH}}|_{u=1} = 24\pi^2.$$

The strict compact channel is defined on the sub-Planckian domain $0 < u \leq 1$ with boundary representative $u_b = 1$. Writing the reduced Planck mass as $\bar{M}_{\mathrm{P}} = \kappa^{-1}$ and the corresponding vacuum potential as $V_\Lambda = \Lambda\bar{M}_{\mathrm{P}}^2$, this condition is exactly

$$V_\Lambda = \bar{M}_{\mathrm{P}}^4.$$

Thus the boundary is the point at which the vacuum potential reaches one reduced-Planck energy density. Within that domain, endpoint dominance selects the boundary member of the saddle family, and its classical exponent is exactly $24\pi^2$. The boundary condition is the physical input; its consequences are fixed. Table 1 records this status. The conformal zero mode has no interior saddle (Appendix C); the alternative R2 modulus reading instead produces a boundary layer of fractional width $1/B$. We use the unreduced Planck mass $M_{\mathrm{P}} = G^{-1/2}$ for the observable $G\Lambda = \Lambda/M_{\mathrm{P}}^2$; the instanton exponent is naturally written in terms of the gravitational coupling $\kappa^2 = 8\pi G$.

The on-shell saddle action and the de Sitter entropy are related by an exact identity. The Bekenstein–Hawking entropy is $S_{\mathrm{dS}} = 3\pi M_{\mathrm{P}}^2/\Lambda$; the on-shell action is $B = 24\pi^2/(\kappa^2\Lambda) = 3\pi M_{\mathrm{P}}^2/\Lambda$. Therefore

$$B = S_{\mathrm{dS}}\,, \tag{23}$$

exact for any Λ. The saddle exponent equals the de Sitter entropy. This identity remains important in recent finite-volume partition-function treatments of gravitational thermodynamics [81]. At the Planck-curvature normalisation $u = 1$ this is the finite Planck-boundary entropy $S_{\mathrm{dS}}|_{u=1} = 24\pi^2 \approx 237$ of the ultraviolet saddle; the observed cosmological constant emerges from the full result Eq. (48), not from this saddle entropy. Thus $e^{-24\pi^2}$ is the Planck-curvature trans-series sector weight, not the Gibbons–Hawking partition function of the observed late-time de Sitter universe, whose entropy would be $S_{\mathrm{dS}} \sim 10^{122}$ with the opposite large-sign weighting in a macroscopic de Sitter partition-function interpretation.

This connection can be placed on rigorous geometric footing. On any conformally flat Einstein 4-manifold, the Chern–Gauss–Bonnet theorem [34] gives

$$|S_{\mathrm{EH}}| = \tfrac{3}{2}\,\chi(M)\ \times\ \frac{8\pi^2}{\kappa^2\Lambda}\,, \tag{24}$$

where $\chi(M)$ is the Euler characteristic. For S^4, $\chi = 2$, recovering $|S_{\mathrm{EH}}| = 24\pi^2/(\kappa^2\Lambda)$. This factorisation through the Euler characteristic is special to four dimensions: the Gauss–Bonnet density is then a four-form, paralleling the four-dimensional Yang–Mills topological density. None of these results involves a contour choice or a dynamical assumption; they are properties of the round-S^4 geometry itself.

Compact representative for the extraction theorem. The extraction map (Theorem 1) requires a conformally flat background ($W_{\mu\nu\rho\sigma} = 0$), because the uniqueness proof (Theorem 1, condition C2) relies on the vanishing of the Weyl tensor. The round S^4 is the admissible compact positive-curvature representative of the universal conformally flat channel used here. Non-spin representatives are inadmissible for the Standard Model fermion determinant, while non-conformally-flat representatives carry W^2 or other non-universal data and are projected out by C2. For example,

$\mathbb{CP}^2$ is not spin and is not conformally flat, while $S^2 \times S^2$ is spin but has $W \neq 0$, so the c-anomaly contributes and the extraction also contains the c anomaly [35]. We require only the narrower claim that round S^4 represents the protected local conformally flat channel, not a classification of all gravitational saddles.

Sourced Feynman/Lefschetz contour. We compute the sourced Lorentzian vacuum functional in the paired-cap curvature-charge coordinate, evaluated in the leading saddle approximation. The suppressed-thimble clause of the compact-channel prescription fixes the original contour and observable so that the compact round-S^4 thimble associated with de Sitter space is included with the decaying orientation $e^{-|S_{\mathrm{EH}}|}$ [59, 60, 77].[1] The source enters analytically and is differentiated before it is set to zero, so it changes the in-sector response but not the classical on-shell action of the compact saddle.

Named contour alternative. The decaying orientation selected here has the same semiclassical exponential sign as the tunnelling, or Vilenkin, de Sitter weighting $\exp[-3\pi/(G\Lambda)]$ [76]. At the selected boundary $\kappa^2\Lambda = 1$,

$$\frac{3\pi}{G\Lambda} = 24\pi^2.$$

The opposite Hartle–Hawking orientation [75] would replace $e^{-24\pi^2}$ by $e^{+24\pi^2}$ and hence enlarge the leading prediction by

$$e^{48\pi^2} \simeq 10^{205.7}.$$

It therefore falsifies this compact channel. This comparison concerns only the sign of the semiclassical compact weight: the paired-cap coefficient defined in Eq. (4) is not identified with a vacuum-decay rate or a universe-creation probability, and the broader contour question remains boundary-condition dependent.

Admissibility under the suppressed-thimble clause. Assume that the defining contour contains the compact round-S^4 thimble with the suppressed weight $e^{-|S_{\mathrm{EH}}|}$. With $\Gamma = -\ln Z$ and the determinant sign fixed in Sec. 4, the reduced scale measure on the declared sub-Planckian domain is proportional to $z^{-2a_{\mathrm{SM}}-1}dz$ with $z = e^{2\sigma_0} \geq 1$. The Planck boundary, not the sign of a_{SM}, removes the small-z endpoint; the damped thimble controls the large-z end. The selected sector is therefore finite on its declared domain and has classical grade $e^{-24\pi^2}$. This check does not independently determine the contour, its orientation, or its Stokes data.

Verification. The physical-domain integral is displayed in Eq. (26). Extending the modulus to $z = 0$ would reintroduce the excluded super-Planckian region and gives the divergent R1 reading; it is not a convergence test passed by $a_{\mathrm{SM}} > 0$.

Endpoint dominance of the sector family. Label the round-S^4 sectors in the declared sub-Planckian domain by $x = M_{\mathrm{P}}^2/H^2 = 1/u \in [1, \infty)$, with classical action $B(x) = 24\pi^2 x$. Since $B(x)$ is strictly increasing, the leading sector is the boundary member $x = 1$. Every interior sector is suppressed by $e^{-24\pi^2(x-1)}$ relative to it, already below 10^{-102} at $x = 2$. Any polynomially bounded modulus measure therefore localises at the boundary with fractional width $1/B \simeq 0.4\%$ (the R2 reading of Sec. 14.2).

[1] This is an observable-specific contour input, not a claim that Picard–Lefschetz theory selects a universal de Sitter contour independently of boundary conditions. It does not settle the global no-boundary contour debate [75]; in particular it is compatible with the Stokes-line issues discussed by Feldbrugge et al. [61], Diaz Dorronsoro et al. [62], and the review [72].

The boundary unit. The selected channel takes $u_b \equiv (\kappa^2\Lambda)_{\text{boundary}} = 1$, the tree-level Planck-curvature boundary in the loop-counting variable $u = \kappa^2\Lambda$. This value is fixed by the tree-level boundary convention, independently of the cosmological value. Other ultraviolet boundary definitions specify quantitatively different models (Appendix D), so observation sharply tests the exact boundary condition. The domain and boundary unit are recorded in Table 1.

The representative sector is treated at leading tree-saddle order at the gravitational boundary; its internal curvature is Planckian because that is the scale assigned to the selected compact de Sitter saddle [59, 60]. It is *not* the observed late-time de Sitter curvature inserted back into the macroscopic Einstein equation, which would be circular. The sourced one-saddle formulation (Sec. 11) makes this distinction precise: $e^{-24\pi^2}$ is the weight of a non-perturbative sector in the trans-series expansion of the sourced partition function, not a self-consistent solution of the classical field equations.

Status of the gravitational saddle weight. At leading saddle order, each included metric saddle is weighted by its on-shell Einstein–Hilbert action while Standard Model matter is quantised on that saddle. Thus $e^{-S_{\text{EH}}}$ is the classical trans-series grade of the compact sector. In the paired-cap response, source-independent metric and ghost determinants cancel against the zero-compensator cap norm. A gravitational determinant that depends on the compensator can dress the response, while higher-curvature operators can modify the complete Planck-boundary action. Those are the outstanding microscopic correction calculations (Appendix A).

Exponential sensitivity and the trans-series structure. Since $B = 24\pi^2 \approx 237$, a shift $\delta B = O(1)$ changes the answer by an order-one factor. The sector expansion displays this sensitivity: B is the classical Einstein–Hilbert action grading the primitive thimble, while the sector-normalised response is a separate coefficient. This is analogous to sector-resolved instanton calculus, but here the external compensator is not the gravitational collective coordinate. Within the Einstein–Hilbert truncation $B = 24\pi^2$; higher-curvature corrections test that exponent. Source-independent determinant normalisations and phases cancel in the cap quotient rather than entering as an unknown multiplicative factor.

Finite curvature-squared terms do not shift the protected source response. On round conformally flat S^4, finite terms in the dimension-four curvature basis contribute either counterterm-degenerate local pieces or H-independent constants to the one-saddle effective action. The Wess–Zumino source derivative annihilates the constants, while C1 removes the counterterm-degenerate pieces. They can change an unprotected partition-function normalisation but not the protected response or the classical Einstein–Hilbert value $B = 24\pi^2$. Higher-curvature operators can alter the complete Planck-boundary saddle action and are a separate UV effect.

The sourced semiclassical contour and the compact saddle geometry yield:

$$e^{-|S_{\text{EH}}|} = e^{-24\pi^2} = 1.344 \times 10^{-103}\,, \tag{25}$$

accounting for 103 of the 122 orders of magnitude. For the corresponding round geometry, the selected suppressed factor has an exponent equal in magnitude to its de Sitter entropy, $e^{-24\pi^2} = e^{-S_{\text{dS}}}$ (Appendix C).

Technical support: zero-mode domain and contour. With the corrected determinant sign, the damped reduced integral on the physical domain $z = e^{2\sigma_0} \geq 1$ is

$$I_{\text{dom}}(C) = \frac{1}{2}\int_1^\infty z^{-2a_{\text{SM}}-1} e^{-Cz}\, dz = \frac{1}{2} C^{2a_{\text{SM}}} \Gamma(-2a_{\text{SM}}, C), \qquad C > 0, \tag{26}$$

where $\Gamma(s,x)$ is the upper incomplete gamma function. The lower limit is the declared Planck boundary; it removes the super-Planckian small-radius region. A Lorentzian representation is obtained by $C \to \epsilon - iC$ and deforming only the large-z end onto a damped ray, without moving the lower endpoint through $z = 0$. Thus the domain controls the finite endpoint and the thimble controls infinity. Extending the integral to $z = 0$ is the inadmissible R1 reading and diverges for $a_{\rm SM} > 0$. This modulus integral is the R2 reading; the cosmological charge instead uses the normalised paired-cap coefficient. The small matter-anomaly ratio $a_{\rm SM}/(24\pi^2) \approx 0.012$, the absence of control over full Planck-scale quantum-gravity corrections, and the non-zero-mode Paneitz term are detailed in Appendix C.

10 Scale selection from endpoint-conjugate cap reflection

The response scale is fixed by the placement of the cap insertion, not by assigning a second curvature to the gravitational saddle. The QCD and Planck endpoint standards define a finite dilation-time interval

$$s \equiv \ln \frac{h}{m_p}, \qquad 0 \le s \le L, \qquad L \equiv \ln \frac{M_{\rm P}}{m_p}. \tag{27}$$

Logarithmic scale is Euclidean transfer time in radial quantisation [100]. The matching hypothesis has two parts. First, the ultraviolet Planck cap state and the infrared stable-proton trace state are posited to be Osterwalder–Schrader-conjugate endpoints of one finite dilation-transfer amplitude. Under this endpoint-conjugacy assumption, the interval carries the reflection

$$\Theta : s \longmapsto L - s. \tag{28}$$

For the matter functional on the fixed Euclidean cap, reflection positivity supplies the real cap norm and the conjugation used in the sector normalisation [98, 99]. Second, the compact charge is represented by the reflection-even local one-point coefficient of the matched UV–IR cap amplitude. The first assumption supplies the reflected interval; the second places the insertion on its fixed plane.

A local scalar insertion invariant under endpoint exchange must lie on the fixed plane of Θ. The fixed point is unique:

$$s_* = \frac{L}{2}, \qquad h_*^2 = m_p M_{\rm P}. \tag{29}$$

In multiplicative variables the same reflection is

$$\mathcal{I} : h \longmapsto \frac{m_p M_{\rm P}}{h}. \tag{30}$$

This involution is the coordinate representation of endpoint-conjugate cap reflection; it is not an independent matching rule.

Endpoint identification. The ultraviolet endpoint is the Planck-boundary representative of the primitive compact thimble. The infrared endpoint must be a scheme-independent, colour-singlet, zero-temperature mass generated by QCD dimensional transmutation and capable of defining an asymptotic stress-tensor charge. For a relativistically normalised proton state, energy–momentum conservation gives

$$\langle p(P)|T^{\mu}{}_{\mu}|p(P)\rangle = 2m_p^2, \tag{31}$$

so the proton pole is directly a physical trace-charge standard [57]. Requiring stability in the full Standard Model selects the proton as the lightest eligible hadronic pole. This does not assert that a one-proton state dominates the vacuum scalar spectral density; it uses m_p as the stable QCD endpoint standard. Appendix D compares nearby alternatives.

On-saddle comparison. Setting $h = H_s = M_\mathrm{P}$ places the external insertion at the ultraviolet end $s = L$ and gives the R0 reading of Sec. 14.2. The paired-cap coefficient is evaluated instead at the reflection plane. Operationally, u_s labels the Lefschetz sector and h labels an external local-RG source within it.

At $h_* = \sqrt{m_p M_\mathrm{P}} \simeq 3.4 \times 10^9$ GeV, Standard Model couplings can be evolved perturbatively, mass-threshold expansions are controlled, and the scale lies in the range analysed in Standard Model vacuum-stability studies [70, 69, 86].

11 Paired-cap response of the primitive sector

The extraction theorem fixes the universal matter datum. We now evaluate its normalised one-cap response in the primitive gravitational sector.

Fixed saddle and external compensator. Let g_s be the round S^4 representative at $u_s = 1$, with $B_s = 24\pi^2$. Introduce a constant compensator τ only in the matter generating functional,

$$\widehat{g}_{\mu\nu}(\tau) = e^{2\tau} g_{s,\mu\nu}, \qquad h = M_\mathrm{P} e^{-\tau}, \qquad x_h = e^{2\tau} = \frac{M_\mathrm{P}^2}{h^2}.$$

This is the standard dilaton/local-RG spurion: τ is an external source for the integrated trace operator and is not integrated as a second metric modulus [45, 95]. The notation $\widehat{g} = e^{2\tau} g_s$ organises the finite Weyl response; the dynamical gravitational representative remains g_s. Its sector action therefore remains B_s while h labels the finite matter-source insertion.

Cut the sphere at its equator. The equator is totally geodesic, the Euler integral on one cap is half the full-sphere value, and the additional boundary-anomaly structures vanish on this conformally flat, totally-geodesic gluing surface [96, 97]. With the determinant-checked convention of Theorem 1, the universal one-cap difference is

$$\Delta\Gamma_{A,+}(h) = 2\mathcal{A}_m(h) \ln \frac{M_\mathrm{P}}{h} = \mathcal{A}_m(h) \ln x_h, \tag{32}$$

up to the separated local-RG threshold and interaction terms.

After the volume direction has been quotiented as the compact vacuum-energy ambiguity, the two-derivative Einstein curvature charge is the only nonconstant local geometric coordinate in the operator basis retained through four derivatives. Six- and higher-derivative directions belong to the correction budget.

Proposition 4 (One-cap curvature-charge response)**.** *On the round cap source family define*

$$\mathcal{C}_+(h) \equiv \frac{1}{4\kappa^2} \int_{D^4_+} d^4x \sqrt{\widehat{g}(h)}\, R[\widehat{g}(h)]. \tag{33}$$

At the primitive boundary $u_s = 1$,

$$\frac{\mathcal{C}_+(h)}{\mathcal{C}_{+,0}} = x_h, \qquad \mathcal{C}_+(h) = 12\pi^2 x_h, \qquad \mathcal{C}_{+,0} = 12\pi^2 = \frac{B_s}{2}. \tag{34}$$

Normalising the conjugate derivative to one primitive cap,

$$\mathcal{D}_+ \equiv \mathcal{C}_{+,0} \frac{d}{d\mathcal{C}_+(h)}, \tag{35}$$

gives

$$\Xi_\mathrm{WZ}(h) \equiv \mathcal{D}_+ \Delta\Gamma_{A,+}(h) = \mathcal{A}_m(h) \frac{h^2}{M_\mathrm{P}^2}. \tag{36}$$

Proof. For $\widehat{g}_{\mu\nu} = x_h g_{s,\mu\nu}$ in four dimensions, $\sqrt{\widehat{g}}\, R[\widehat{g}] = x_h \sqrt{g_s} R[g_s]$. Hence $\mathcal{C}_+/\mathcal{C}_{+,0} = x_h$. At $u_s = \kappa^2 \Lambda_s = 1$,

$$\mathcal{C}_{+,0} = \frac{1}{4\kappa^2} \int_{D^4_+} \sqrt{g_s} R[g_s] = 12\pi^2,$$

which equals the magnitude of the on-shell Einstein–Hilbert action of one reference cap. Since $\Delta\Gamma_{A,+} = \mathcal{A}_m \ln(\mathcal{C}_+/\mathcal{C}_{+,0})$,

$$\mathcal{C}_{+,0} \frac{d\Delta\Gamma_{A,+}}{d\mathcal{C}_+} = \mathcal{A}_m \frac{\mathcal{C}_{+,0}}{\mathcal{C}_+} = \mathcal{A}_m \frac{h^2}{M_{\mathrm{P}}^2}.$$

The cap integral is additive under gluing, and its normalisation is fixed by the primitive reference cap. Any constant rescaling of $\mathcal{C}_+$ cancels between $\mathcal{C}_{+,0}$ and $d/d\mathcal{C}_+$; the response depends on the linear Weyl scaling of the charge, not on its displayed overall normalisation. □

The charge $\mathcal{C}_+$ is a coordinate on the external source family, not an additive term in the extracted matter functional; finite $\int \sqrt{g}R$ counterterms remain excluded by the Euler projector. It is also not the complete off-shell Einstein–Hilbert action at fixed Λ_s, which contains a volume term scaling as x_h^2. The dynamical saddle and its classical grade remain fixed at $u_s = 1$.

Sector-normalised primitive coefficient. Using Eq. (4), define

$$\Delta\Gamma_{n,+}(h \,|\, u_s) = -\ln \frac{Z_{n,+}(h \,|\, u_s)}{Z_{n,+}(M_{\mathrm{P}} \,|\, u_s)}. \tag{37}$$

The same reflected bra appears in both matrix elements, so its overall normalisation and phase cancel. The ratio also removes all other factors independent of h, including finite local constants, collective-coordinate volumes and source-independent determinants. Source-dependent quantum terms remain and contribute to $\mathcal{A}_m(h)$ or to the correction budget.

The leading primitive contribution is therefore

$$q_{\mathrm{WZ}}(h) = e^{-B_s} \mathcal{D}_+ \Delta\Gamma_{1,+}(h \,|\, 1) + O(e^{-2B_s}). \tag{38}$$

Here e^{-B_s} grades the chosen gravitational sector, while the normalised cap ratio supplies its connected matter response. The optional replica bookkeeping that isolates this coefficient from a multi-sector series is given in Appendix A.

Reflection-point evaluation. Equation (29) gives

$$\frac{h_*^2}{M_{\mathrm{P}}^2} = \frac{m_p}{M_{\mathrm{P}}}.$$

Combining the primitive sector weight, the cap curvature-charge response and the reflection point gives the strict result. Equivalently, $h_*^2/M_{\mathrm{P}}^2 = S_{\mathrm{dS}}(M_{\mathrm{P}})/S_{\mathrm{dS}}(h_*)$.

Proposition 5 (Strict-channel compact response)**.** *For the primitive suppressed round-S^4 sector, the normalised one-cap curvature-charge response and the two-part matching hypothesis imply*

$$q_{\mathrm{WZ}} = a_{\mathrm{eff}}(h_*) \frac{h_*^2}{M_{\mathrm{P}}^2} e^{-24\pi^2} + O(e^{-2B_s}) + O\!\left(\frac{m_i^2}{h_*^2}\right). \tag{39}$$

At leading Standard Model order, $a_{\mathrm{eff}}(h_*) = a_{\mathrm{SM}} = 1991/720$, and

$$\boxed{q_{\mathrm{WZ}} = a_{\mathrm{SM}} \frac{m_p}{M_{\mathrm{P}}} e^{-24\pi^2} = 2.856 \times 10^{-122}.} \tag{40}$$

Proof. The primitive thimble supplies $e^{-B_s} = e^{-24\pi^2}$. Theorem 1 and Eq. (32) give the one-cap Euler functional. Proposition 4 gives its positive one-cap curvature-charge slope $\mathcal{A}_m(h)h^2/M_{\rm P}^2$. Under the two-part matching hypothesis, endpoint conjugacy supplies the reflection and reflection-even readout fixes its plane, giving $h_*^2/M_{\rm P}^2 = m_p/M_{\rm P}$. Source-independent determinants and common phases have already cancelled in Eq. (37). □

12 Global-source completion

Dimensionless-source action. For a connected finite-volume representative define

$$\langle X\rangle = \frac{\int_M \sqrt{|g|}\, X\, d^4x}{\int_M \sqrt{|g|}\, d^4x}.$$

The compact calculation supplies the rigid dimensionless number $q_{\rm WZ}$. We write the action directly in terms of the rigid dimensionless charge $q_{\rm WZ}$, with the independent variables fixed before variation:

$$S_{\rm gs} = \int_M \left[\left(\frac{\mathcal{P}^2}{2}R - \mathcal{L}_m\right)\star 1 + \Lambda_b(F_4 - \star 1) - 8\pi(\mathcal{P}^2)^2 q_{\rm WZ} F_4\right]. \tag{41}$$

Here $\mathcal{P}^2$ is rigid, with physical branch $\mathcal{P}^2 = M_{\rm P}^2/(8\pi)$, $F_4 = dA_3$ is an auxiliary closed four-form in a fixed nonzero cohomology class, and $q_{\rm WZ}$ is held fixed under the rigid $\mathcal{P}^2$ variation. The coefficient 8π implements directly the convention $q_{\rm WZ} = G\Lambda$ with $G = (8\pi\mathcal{P}^2)^{-1}$. Its minus sign is the standard Legendre pairing between the positive cap charge $q_{\rm WZ} = e^{-B_s}\mathcal{D}_+\Delta\Gamma_{1,+}$ and its global source: the Legendre functional contains minus source times conjugate charge. The coefficient and sign are fixed at the action level by this source–charge convention. The action adds no local propagating degree of freedom. It is of Henneaux–Teitelboim and manifestly local sequestering type [39, 40, 41].

Coefficient and ordering audit. Replace the coefficient 8π in Eq. (41) by a general dimensionless constant c. The rigid variation then gives

$$\frac{\langle R\rangle}{4M_{\rm P}^2} = \frac{c}{8\pi}q_{\rm WZ}, \qquad \frac{\Lambda}{M_{\rm P}^2} = \frac{c}{8\pi}q_{\rm WZ} \quad (T_{\mu\nu} = 0).$$

The compact charge is defined in the observable convention $q_{\rm WZ} = G\Lambda$, with $G = (8\pi\mathcal{P}^2)^{-1}$; this source–charge convention sets $c = 8\pi$. The sign is set by the Legendre orientation stated above. This direct dimensionless action is not obtained by substituting a relation $\mathcal{Q} = M_{\rm P}^2 q_{\rm WZ}$ into a different action before variation, so the factor-of-two alternative belongs to a different source functional rather than to an ordering ambiguity in Eq. (41).

Theorem 6 (Compact global-source completion)**.** *The variations of Eq. (41) imply*

$$\boxed{\frac{\langle R\rangle}{4M_{\rm P}^2} = q_{\rm WZ},} \tag{42}$$

and

$$\boxed{G_{\mu\nu} + M_{\rm P}^2 q_{\rm WZ} g_{\mu\nu} = \frac{8\pi}{M_{\rm P}^2}\left(T_{\mu\nu} - \frac{1}{4}\langle T\rangle g_{\mu\nu}\right).} \tag{43}$$

The local traceless projection is Eq. (17); constant shifts of the matter Lagrangian cancel exactly. On a maximally symmetric vacuum,

$$\boxed{\frac{\Lambda}{M_{\rm P}^2} = q_{\rm WZ}.} \tag{44}$$

Proof. Variation of Λ_b gives $F_4 = \star 1$. Variation of A_3 gives $d[\Lambda_b - 8\pi(\mathcal{P}^2)^2 q_{\rm WZ}] = 0$, so Λ_b is spacetime constant on a fixed branch. Varying $y \equiv \mathcal{P}^2$ at fixed $q_{\rm WZ}$ gives

$$\frac{1}{2}\int_M R \star 1 - 16\pi y q_{\rm WZ} \int_M F_4 = 0.$$

Using $F_4 = \star 1$ after variation yields

$$\langle R \rangle = 32\pi \mathcal{P}^2 q_{\rm WZ} = 4M_{\rm P}^2 q_{\rm WZ},$$

which proves Eq. (42). Metric variation, with F_4 metric independent off shell, gives

$$\mathcal{P}^2 G_{\mu\nu} + \Lambda_b g_{\mu\nu} = T_{\mu\nu}.$$

Averaging its trace and using the sum rule gives

$$\Lambda_b = 8\pi(\mathcal{P}^2)^2 q_{\rm WZ} + \frac{1}{4}\langle T \rangle.$$

Substitution and $\mathcal{P}^2 = M_{\rm P}^2/(8\pi)$ yield Eq. (43). The traceless projection is Eq. (17); under $T_{\mu\nu} \mapsto T_{\mu\nu} - \rho g_{\mu\nu}$ the two terms in the parenthesis shift equally and cancel. For $T_{\mu\nu} = 0$ and $R_{\mu\nu} = \Lambda g_{\mu\nu}$, Eq. (44) follows. □

Residual equation of state. On a fixed global-source branch, both $q_{\rm WZ}$ and the global number $\langle T \rangle$ are spacetime constants. Equation (43) can therefore be written

$$G_{\mu\nu} + \Lambda_{\rm res} g_{\mu\nu} = \frac{8\pi}{M_{\rm P}^2} T_{\mu\nu}, \qquad \Lambda_{\rm res} \equiv M_{\rm P}^2 q_{\rm WZ} + \frac{2\pi}{M_{\rm P}^2}\langle T \rangle. \tag{45}$$

The residual term is exactly proportional to $g_{\mu\nu}$ and therefore obeys $p_{\rm res} = -\rho_{\rm res}$, so $w_{\rm res} = -1$ at finite redshift as well as asymptotically wherever it is identified with dark energy. This statement follows from the proposed four-form completion, not from the compact anomaly extraction theorem. It does not require $\langle T \rangle = 0$: the trace-average condition fixes the residual amplitude, not its equation of state.

Specifying the coupling directly at action level removes any factor-of-two ordering ambiguity. The independent variables are $\mathcal{P}^2$, Λ_b, F_4, and the rigid dimensionless number $q_{\rm WZ}$; the variation is performed at fixed $q_{\rm WZ}$. Substituting $M_{\rm P}^2 = 8\pi\mathcal{P}^2$ only after variation is then an identity, not a matching prescription. Reversing the sign of the last term would be a different Legendre orientation and would contradict the definition of $q_{\rm WZ}$ as the positive conjugate cap response.

On round S^4 the local anomaly stress is homogeneous, $T^A_{\mu\nu} = C g_{\mu\nu}$, and therefore cancels exactly from $T_{\mu\nu} - \langle T \rangle g_{\mu\nu}/4$. The unwanted local H^4 backreaction is not counted a second time. Nonhomogeneous anomaly stresses and ordinary finite-wavelength matter excitations continue to gravitate through Eq. (43), while the protected compact datum survives separately in $q_{\rm WZ}$.

From the compact theorem to the observed late-time branch. For a cosmology with a matter history, local late-time vacuum does not by itself imply $\langle T \rangle = 0$. The direct observational identification uses a regulated Lorentzian continuation on domains M_τ and assumes

$$\langle T \rangle_{\rm reg} \equiv \lim_{\tau\to\infty} \frac{\int_{M_\tau} \sqrt{-g}\, T_{\rm nonvac}\, d^4x}{\int_{M_\tau} \sqrt{-g}\, d^4x} = 0. \tag{46}$$

This holds for a future-eternal asymptotically de Sitter branch whenever the integrated non-vacuum trace grows more slowly than the four-volume, as for ordinary diluted matter of finite comoving abundance; radiation is trace-free. Under Eq. (46), the asymptotic vacuum curvature obeys

$$\frac{\Lambda_\infty}{M_{\rm P}^2} = q_{\rm WZ}. \tag{47}$$

If the regulated average does not vanish, the completed equation instead gives $\Lambda_\infty = M_{\rm P}^2 q_{\rm WZ} + 2\pi\langle T\rangle_{\rm reg}/M_{\rm P}^2$. This shift is also spacetime constant, so it changes the amplitude of the residual source but not its equation of state. Equation (46) is therefore an explicit amplitude condition used in the numerical comparison, not a consequence of the compact Euclidean extraction theorem.

Corollary (asymptotic cosmological value). Combining the compact response Eq. (40) with Eq. (47) gives

$$\boxed{\frac{\Lambda_\infty}{M_{\rm P}^2} = q_{\rm WZ} = a_{\rm SM}\,\frac{m_p}{M_{\rm P}}\,e^{-24\pi^2} = 2.856\times 10^{-122}.} \tag{48}$$

Explicitly,

$$\frac{\Lambda_\infty}{M_{\rm P}^2} = 2.76528 \times 7.685 \times 10^{-20} \times 1.344 \times 10^{-103} = 2.856 \times 10^{-122}. \tag{49}$$

The Planck 2018 flat-ΛCDM-inferred value is $(\Lambda/M_{\rm P}^2)_{\rm obs} = (2.846\pm 0.057)\times 10^{-122}$, a 0.4% difference in central value. This comparison is conditional on the flat-ΛCDM inference. If the observed acceleration is established as evolving, the quoted value is not a direct measurement of the asymptotic constant Λ_∞ predicted here. No parameter is fitted to the cosmological value once the stated channel clauses, global-source action, and asymptotic condition are imposed. In inverted form, $a_{\rm inf} = 2.755 \pm 0.055$ against $a_{\rm SM} = 2.76528$.

13 Correction budget, predictions, and tests

The paired-cap ratio removes source-independent normalisations rather than setting them to unity. The remaining corrections divide into matter-response corrections, ultraviolet changes to the primitive action, higher primitive sectors, and robustness tests of the endpoint rule.

Interaction corrections to $a_{\rm SM}$. The field-count value $a_{\rm SM} = 1991/720$ is the leading fixed-point result. Local-RG and interacting-ϕ^4 calculations support strong suppression of the first physical Euler-coefficient correction in the examples presently controlled, but no complete curved-space Standard Model result at h_* is available (Sec. 5). The broader source-dependent cap determinant can receive two-loop curved-background contributions of order $g^2/(16\pi^2)$. At $h_* \simeq 3.4\times 10^9$ GeV the top Yukawa gives the largest simple estimate, $y_t^2/(16\pi^2) \simeq 0.2\%$; we retain $\lesssim 0.5\%$ as a provisional matter-response estimate, not a calculated uncertainty. A complete Standard Model two-loop cap calculation would replace it. The interacting curved-space anomaly analysis of Fröb and Zahn provides a relevant structural check [67].

Determinants, phases, and ultraviolet action corrections. Any factor independent of the compensator cancels exactly in Eq. (37); this includes a common sphere phase and source-independent metric/ghost determinants. This is an observable quotient, not a unit-prefactor assumption. A determinant that depends on the compensator contributes to the response and is included in the matter or gravitational-dressing correction. Higher-curvature operators can change

Table 3: Correction and robustness budget. Source-independent normalisations and common phases cancel by definition of the paired cap response; they are not fitted factors.

Source	Size	Status
Field-count value of a_{SM}	exact at free fixed point	rational
Free-scalar sign and normalisation	exact	determinant checked
SM mass thresholds	$\lesssim 3 \times 10^{-15}$	negligible
Interaction/source response	$\lesssim 0.5\%$	estimated
Source-independent determinants/phases	cancel	exact quotient
Higher primitive sectors	$O(e^{-24\pi^2})$ relative	negligible barring enhancement
Higher-curvature shift of B_s	not quantified	ultraviolet test
Source-dependent gravitational dressing	not quantified	beyond matter-QFT truncation
Endpoint-rule relaxation	$\sim$4%	robustness test
Estimated matter-response envelope	$\lesssim$ **0.5%**	estimated

the primitive action B_s itself. Because the exponential is sensitive to δB_s, this is the principal ultraviolet calculation still required; no numerical error is assigned before a UV completion is specified. Higher primitive sectors are suppressed by at least another factor e^{-B_s} unless their coefficients grow exponentially.

Endpoint-scale sensitivity. The selected endpoint is the proton pole, selected by the trace-charge, colour-singlet, zero-temperature and stability criteria. A nearby thermal diagnostic, $2\pi T_c \simeq 974$ MeV [55], differs from m_p by about 4% but fails the pole and stability criteria. The comparison is therefore a robustness test of changing the endpoint rule, not an uncertainty within the proton prescription.

Correction and robustness budget. The displayed uncertainty on $a_{\mathrm{inf}} = 2.755 \pm 0.055$ is observational, not a theoretical error bar. Within the stated Einstein–Hilbert paired-cap channel, the leading result differs from the flat-ΛCDM central value by 0.4% (0.18σ). The ultraviolet action test and the separate endpoint robustness test are not folded into that observational uncertainty.

Hadronic endpoint selection. The infrared endpoint of the zero-temperature sourced gravitational functional must be a colour-singlet, RG-invariant physical pole mass that remains stable in the full Standard Model and therefore carries the QCD trace anomaly into late-time macroscopic physics. This criterion excludes Λ_{QCD} (a scheme-dependent running parameter rather than a pole mass), pions (pseudo-Goldstone and unstable), and the pure-Yang–Mills glueball scale (not a full-Standard-Model asymptotic pole). The proton is the lightest stable hadronic pole meeting all of these requirements [4]. Table 4 quantifies the numerical sensitivity once this selection criterion is relaxed.

The hadron masses and stability assignments are rounded from the 2026 Review of Particle Physics [4]; the crossover entry uses Ref. [55], and the 0^{++} pure-Yang–Mills proxy uses Ref. [56].

The proton is therefore the physically distinguished endpoint: it is the lightest stable hadronic pole, survives to late cosmological times, and is the first asymptotic QCD state that can source macroscopic gravity through a renormalised stress tensor. The neutron and η' lie numerically close to the strict result but fail the stability criterion; their inclusion makes explicit that numerical proximity is not the endpoint rule. Table 4 quantifies the sensitivity around this selection; the candidates are not equally eligible, since only the proton satisfies all three criteria.

Table 4: IR endpoint candidates scored against the strict endpoint criteria. A candidate must be a scheme-independent pole mass (P), stable in the full Standard Model (S), and a colour singlet (C). Counterterm invariance motivates the physical-pole requirement; stability and colour-singlet character are additional channel criteria. Only the proton satisfies all three; $2\pi T_c$ is a thermal crossover diagnostic rather than a pole mass (Sec. 10).

Candidate	Mass (GeV)	P	S	C	$\Lambda_{\text{pred}}/\Lambda_{\text{obs}}$	Dev.
m_π (pion)	0.140	✓	×	✓	0.150	−85%
$\Lambda^{(3)}_{\overline{\text{MS}}}$	0.332	×	n/a	n/a	0.355	−64%
m_ρ (rho)	0.775	✓	×	✓	0.829	−17%
m_p (proton)	0.938	✓	✓	✓	1.004	+0.4%
m_n (neutron)	0.940	✓	×	✓	1.005	+0.5%
$m_{\eta'}$	0.958	✓	×	✓	1.025	+2.5%
$2\pi T_c$	0.974	×	n/a	n/a	1.042	+4.2%
$m^{\text{YM}}_{0^{++}}$	~ 1.7	×	n/a	✓	~ 1.82	+82%

13.1 Conditional particle-content dependence

Within the leading Einstein–Hilbert paired-cap truncation, the extracted anomaly coefficient makes the predicted Λ depend directly on the active particle content. In the comparison between the inferred coefficient a_{inf} and the particle-counting value a_{SM}, the former is fixed by the measured Λ, while the latter moves with the active field content, so changes in that content can drive the two apart. Table 5 gives representative weakly coupled free-field shifts. The anomaly coefficient is evaluated at $h_* \approx 3.4 \times 10^9$ GeV. In a physical decoupling scheme, a weakly coupled species with $m \ll h_*$ approaches its standard free-field contribution, while a species with $m \gg h_*$ is removed through power-suppressed threshold functions [52]; strongly coupled sectors require a separate calculation.

The field-content test is therefore a test of the leading semiclassical matter-QFT channel. In this channel the active coefficient is the matter type-A anomaly evaluated at $h_* \approx 3.4 \times 10^9$ GeV, with gravity retained at leading saddle order and metric fluctuation effects omitted. Weakly coupled species below h_* shift $a_{\text{eff}}(h_*)$ by their standard free-field coefficients, while species above h_* decouple from the compact matter determinant. A strongly coupled hidden sector, or a UV completion in which metric fluctuations gravitationally dress the anomaly coefficient, would not be a small correction inside the present calculation; it would define an enlarged channel with a different a_{eff}, and the compact-residue comparison would then test that enlarged field content rather than the minimal Standard Model value. The dependence is a conditional sensitivity rather than a standalone BSM exclusion. Once source-dependent gravitational dressing and the higher-curvature correction to the primitive action are controlled, agreement would disfavor additional active weakly coupled matter below the evaluation scale. Source-independent determinant factors cannot compensate such a shift because they cancel in the paired-cap response. This is analogous in spirit to effective-gravity and high-scale SM-stability analyses that turn explicit field-content assumptions into conditional constraints on beyond-Standard- Model sectors [79, 86].

A fourth generation (+8.3%) or low-energy supersymmetry (+18%) would shift the leading-channel prediction substantially. They would be in strong tension with the observed Λ once the source-dependent gravity and ultraviolet-action corrections are controlled below those shifts. The anomaly coefficient is evaluated at $h_* \approx 3.4 \times 10^9$ GeV, so the active field content at that scale must still be exactly the one entering the extraction theorem. One realisation is that any right-handed neutrinos are heavy Majorana states with threshold above h_* and therefore decouple from the effective action

Table 5: Conditional effect of BSM particles on $a_{\rm SM}$ in the leading Einstein–Hilbert paired-cap channel. Interpreting the observed Λ via Eq. (1) gives an inferred window $a_{\rm inf} = 2.755 \pm 0.055$ (i.e. $\pm 2.0\%$) for the proton endpoint; relaxing the endpoint criterion gives a separate $\sim 4\%$ robustness envelope. These shifts become exclusions once source-dependent gravitational dressing and the ultraviolet correction to the primitive action are controlled. [a]15 Weyl fermions per generation (see the field-content table in Appendix B). [b]94 real scalars (sfermions + 2nd Higgs doublet) + 16 Weyl (gauginos + Higgsinos).

Scenario	Δa	$a_{\rm matter}$	Shift
SM (baseline)	n/a	2.765	n/a
$+3\ \nu_R$	33/720	2.811	+1.7%
+1 scalar	2/720	2.768	+0.1%
+1 gen.[a]	165/720	2.994	+8.3%
+MSSM[b]	≈364/720	≈3.27	+18%

at the evaluation scale. In that case the active field content remains the Standard Model's 45 Weyl fermions. Conversely, confirmation of light Dirac neutrinos would shift $a_{\rm SM}$ by +1.7%, using a large fraction of the narrower proton-endpoint observational window and providing a potential test once the endpoint, interaction, source-dependent gravity and ultraviolet-action corrections are controlled.

13.2 Predictions and tests

Dark-energy equation of state. The compact anomaly extraction theorem does not determine an equation of state. The proposed four-form completion does: on any fixed branch, Eq. (45) contains no dynamical dark-energy degree of freedom and predicts a spacetime-constant residual source, $p_{\rm res} = -\rho_{\rm res}$ and hence $w(z) = -1$ (equivalently $w_0 = -1$, $w_a = 0$), at finite redshift as well as asymptotically wherever that source is identified with the observed acceleration. Equation (46) fixes its amplitude, not this equation of state.

DESI DR2 is well described by flat ΛCDM, but combinations with CMB and supernova data show dataset-dependent 2.8–4.2σ preferences for the region $w_0 > -1$, $w_a < 0$; the full six-year DES multi-probe analysis finds 2.3–3.2σ departures across its tested combinations [63, 64]. These results are a material tension, but remain dependent on the datasets and the $w_0 w_a$ parameterisation. Persistent cross-dataset and systematics-robust evidence for evolving dark energy across flexible parametric and non-parametric reconstructions would falsify the proposed global-source completion or the identification of the observed acceleration with its residual constant, while leaving the compact extraction theorem intact.

Boundary-unit sensitivity. The selected channel fixes $u_b = 1$ by the reduced-Planck energy-density condition $V_\Lambda = \bar{M}_{\rm P}^4$, independently of the cosmological value. Because $B = 24\pi^2/u_b$, a fractional shift δ of the exponent changes the central value by $e^{-24\pi^2\delta}$; the $\sim 4\%$ comparison window corresponds to $|\delta| \lesssim \ln(1.04)/(24\pi^2) \approx 2 \times 10^{-4}$. The numerical result is therefore a sharp test of this exact boundary condition.

Field-content dependence. Once source-dependent gravitational dressing and the higher-curvature correction to B_s are controlled below the relevant shift, active weakly coupled particles that alter $a_{\rm eff}(h_*)$ without the corresponding change in Λ would exclude the minimal Standard Model channel. Until then this remains a conditional sensitivity.

14 Discussion

14.1 Status and microscopic completion

The theorem layer and the cosmological completion should be kept distinct. The compact theorem isolates the Euler coefficient and the local-gravity analysis shows why its ordinary metric stress cannot generate a small curvature. The paired-cap construction then defines a scalar two-argument observable: u_s labels the gravitational saddle and h labels an external trace source on that saddle. Its one-cap curvature-charge derivative gives the hierarchy factor, conditional on the two-part matching hypothesis of endpoint conjugacy and reflection-even readout.

The four-form action assigns the compact charge to the scalar curvature mode omitted by the trace-free equation. Its variation cancels constant shifts of the matter Lagrangian and gives a fixed-branch residual source with $w = -1$.

The remaining tests concern the physical completion: whether the quantum-gravity contour contains the suppressed primitive thimble, whether its exact boundary is $u_b = 1$, whether the Planck and proton trace states are endpoint-conjugate, whether the compact charge is the reflection-even local one-point coefficient, and whether the four-form action is the correct global completion. Higher-curvature terms can shift the saddle action and source-dependent determinants can dress the cap response. These effects are part of the correction budget.

The completed equation leaves local QCD dynamics active. Homogeneous constants cancel from $T_{\mu\nu} - \langle T\rangle g_{\mu\nu}/4$, while transitions, interfaces and inhomogeneous stresses continue to gravitate. The construction is therefore closest to trace-free gravity and local sequestering [68, 40, 41, 42, 83], but supplies a specific compact candidate for the residual curvature datum.

14.2 Inequivalent readings of the compact channel

Four quantitative readings must be distinguished. The first three treat the matter scale as the curvature modulus itself. The fourth is the paired-cap coefficient defined in Sec. 11. In the inverse-curvature modulus $x = M_{\rm P}^2/H^2$, with $B = 24\pi^2$, the corrected reduced measure is $x^{-2a_{\rm SM}-1}e^{-Bx}\,dx$.

(R1) Unbounded modulus integral, $x \in (0,\infty)$:

$$I_{\rm R1} = \frac{1}{2}\int_0^\infty x^{-2a_{\rm SM}-1}e^{-Bx}\,dx.$$

For $a_{\rm SM} > 0$ this diverges at $x = 0$, precisely the super-Planckian region excluded by the physical domain. A value assigned by analytic continuation would be contour- and prescription-dependent and is not an admissible compact observable.

(R2) Bounded-window integral, $x \in [1, (M_{\rm P}/m_p)^2]$:

$$I_{\rm R2} \simeq \frac{e^{-B}}{2B}\left[1 - \frac{2a_{\rm SM}+1}{B} + O(B^{-2})\right],$$

which is localised at the ultraviolet boundary and gives $I_{\rm R2} = 2.8 \times 10^{-106}$, about 10^{16} times the observed value.

(R0) On-saddle identification, $h = H_s = M_{\rm P}$:

$$q_{\rm WZ}^{\rm (R0)} = a_{\rm SM}e^{-24\pi^2} \simeq 3.7 \times 10^{-103}.$$

Table 6: The four readings. R1, R2, and R0 identify the response with the curvature-modulus family. R3 is the paired, sector-normalised cap coefficient.

Reading	Weight	Response location	Λ/M_{P}^2
R1: unbounded integral	divergent	excluded $x=0$ endpoint	inadmissible
R2: bounded window	e^{-B}/B	UV boundary	2.8×10^{-106}
R0: on-saddle	e^{-B}	$h=M_{\mathrm{P}}$	$\sim 10^{-103}$
R3: paired cap	e^{-B}	reflection plane	2.86×10^{-122}

This is the result if the external compensator scale is identified with a second name for the saddle curvature. It is not the paired-cap observable: the insertion lies at the UV endpoint and is not fixed under endpoint exchange.

(R3) Reflection-matched paired-cap coefficient:

$$q_{\mathrm{WZ}}^{(\mathrm{R3})} = e^{-24\pi^2}\left[\mathcal{C}_{+,0}\frac{d\Gamma_{A,+}}{d\mathcal{C}_+}\right]_{h=h_*} = a_{\mathrm{SM}}\frac{m_p}{M_{\mathrm{P}}}e^{-24\pi^2}.$$

Here the exponential grades the primitive UV thimble, while the matter factor is a separately defined, sector-normalised cap response. The position $h_*^2 = m_p M_{\mathrm{P}}$ is the fixed plane of endpoint-exchange reflection.

The first three readings treat the matter scale as the curvature modulus. The paired-cap coefficient is a different observable: it holds the primitive gravitational sector fixed and differentiates a normalised matrix element with respect to an external trace source. This distinction is defined by Eqs. (4)–(6), rather than by assigning two values to one modulus. Detailed source and evaluation-point swap tests are collected in the technical appendix.

15 Conclusion

After finite local counterterms are quotiented out on conformally flat S^4, the type-A anomaly coefficient is the unique nonvanishing scheme-independent datum in the local linear constant-Weyl response. With $\Gamma = -\ln Z$,

$$\mathcal{A}[\Gamma] = -\frac{1}{4}\Pi_{H^0}\frac{d\Gamma}{d\ln H} = a,$$

and the conformal-scalar determinant gives $d\Gamma/d\ln H = -1/90 = -4a_s$. Ordinary metric variation still produces an H^4 stress and no small-curvature branch.

The compact channel is defined by the paired cap amplitude

$$Z_+(h\,|\,u_s) = \langle\Omega_-(u_s)|U_h|\Psi_+^{(h)}(u_s)\rangle,$$

its zero-source-normalised logarithm, and the one-cap curvature-charge derivative. The primitive Planck-boundary saddle supplies $e^{-24\pi^2}$. Under the two-part matching hypothesis of endpoint conjugacy and reflection-even readout, the insertion lies on the fixed plane $h_*^2 = m_p M_{\mathrm{P}}$, and the cap response then gives $h_*^2/M_{\mathrm{P}}^2 = m_p/M_{\mathrm{P}}$. At leading Standard Model order,

$$\boxed{q_{\mathrm{WZ}} = a_{\mathrm{SM}}\frac{m_p}{M_{\mathrm{P}}}e^{-24\pi^2} = 2.856\times10^{-122}, \qquad a_{\mathrm{SM}} = \frac{1991}{720}.}$$

The on-saddle and modulus-integral readings are distinct observables and do not reproduce this scale.

The normalised cap ratio removes source-independent determinant factors, zero-mode volumes, finite local constants and common phases. Source-dependent quantum corrections and higher-curvature changes to the primitive action remain calculable tests.

The proposed four-form action supplies the scalar-curvature equation,

$$\frac{\langle R\rangle}{4M_{\mathrm{P}}^2} = q_{\mathrm{WZ}}, \qquad G_{\mu\nu} + M_{\mathrm{P}}^2 q_{\mathrm{WZ}} g_{\mu\nu} = \frac{8\pi}{M_{\mathrm{P}}^2}\left(T_{\mu\nu} - \frac{1}{4}\langle T\rangle g_{\mu\nu}\right).$$

On a maximally symmetric vacuum, $\Lambda/M_{\mathrm{P}}^2 = q_{\mathrm{WZ}}$. On a fixed branch the residual source is constant and has $w = -1$. The regulated non-vacuum trace-average condition fixes the late-time amplitude, not the equation of state.

Under that condition,

$$\frac{\Lambda_\infty}{M_{\mathrm{P}}^2} = 2.856 \times 10^{-122}.$$

The Planck 2018 flat-ΛCDM inference is $(2.846 \pm 0.057) \times 10^{-122}$, so the central values differ by 0.4% (0.18σ). This comparison is conditional on constant Λ; robust evidence for evolving dark energy would challenge the global-source completion or its identification with the observed acceleration, while leaving the compact extraction theorem intact.

The decisive open calculations are the ultraviolet derivation of the suppressed thimble and exact boundary, the source-dependent gravitational dressing of the cap response, and microscopic derivations of the two-part paired-cap matching and the global four-form source.

Acknowledgements

No external funding supported this work.

The author declares no competing financial interest.

Data Availability

No original data were generated. Numerical inputs are taken from the published sources cited in the text.

A Sector normalisation and determinant audit

At fixed u_s, let $Z_{n,+}(h)$ denote the reduced scalar paired-cap matrix element defined in Eq. (4); the corresponding full sector amplitude is $\mathcal{Z}_{n,+}^{\mathrm{full}} = e^{-nB(u_s)} Z_{n,+}$. Factor the reduced matrix element as

$$Z_{n,+}(h) = \mathcal{N}_{n,+} e^{i\phi_{n,+}} \widehat{Z}_{n,+}(h), \tag{50}$$

where $\mathcal{N}_{n,+}$ includes the common overall normalisation of the reflected bra and $\phi_{n,+}$ its common phase; both are independent of the external compensator. The boundary functional of the bra remains in $\widehat{Z}_{n,+}(h)$ and continues to define the conditional matrix element. The sector-resolved connected difference is

$$\Delta\Gamma_{n,+}(h) = -\ln \frac{Z_{n,+}(h)}{Z_{n,+}(M_{\mathrm{P}})} = -\ln \frac{\widehat{Z}_{n,+}(h)}{\widehat{Z}_{n,+}(M_{\mathrm{P}})}. \tag{51}$$

Thus source-independent metric and ghost determinants, collective-coordinate Jacobians, zero-mode volumes, finite local constants, cap-norm magnitudes and common phases cancel identically. Finite R^2 and Euler counterterms that evaluate to constants on the round cap disappear for the same reason.

The marked functional is not the logarithm of an unnormalised sum over saddles. It is generated by the replica-marked conditional functional

$$\mathcal{R}_+(\alpha; h, \zeta \,|\, u_s) = \sum_{n\geq 1} \zeta^n e^{-nB(u_s)} \left[\frac{Z_{n,+}(h \,|\, u_s)}{Z_{n,+}(M_\mathrm{P} \,|\, u_s)}\right]^\alpha, \qquad \mathfrak{d}_+^{\mathrm{mark}} = -\,\partial_\alpha \mathcal{R}_+|_{\alpha=0}\,. \tag{52}$$

Taking $[\zeta]\mathcal{D}_+$ therefore extracts the primitive classical action grade times its conditioned connected response. An unknown relative partition-function normalisation or a common Polchinski-type phase is not silently assigned the value one; it is quotient data and is absent from the marked observable coupled to the global source. The selected damped contour fixes the positive classical grade, while cap conjugation fixes the reality of the conditional matter response.

Three effects remain. A determinant that depends on the compensator contributes to $\mathcal{D}_+\Delta\Gamma$; higher-curvature operators can change B_s; and additional marked sectors generate the explicit $O(e^{-2B_s})$ terms. These are physical corrections. Unnormalised gravity sphere partition functions can indeed carry nontrivial prefactors and phases [48, 49, 87, 89, 92]; Eq. (51) states why those source-independent quantities do not enter the connected cap response.

A.1 Detailed logical-status ledger

A.2 Source and evaluation-point audit

Let $r \equiv m_p/M_P$. The following swaps show the sensitivity of the selected response while keeping the alternatives outside the main argument.

B Standard Model field content and anomaly coefficients

Table 9 lists the per-field a-anomaly coefficients and the Standard Model counting used in Eq. (13).

Hence

$$a_\mathrm{SM} = \frac{8 + 495 + 1488}{720} = \frac{1991}{720}. \tag{53}$$

Common additions give, in units of 1/720: one real scalar +2, one Weyl fermion +11, one vector +124, three right-handed neutrinos +33, and one additional fermion generation +165. These numbers are field-content changes to the compact Euler residue. Their conversion into exclusions is conditional on the global-source action and on control of source-dependent gravitational dressing and higher-curvature changes to the primitive action.

C Conformal zero-mode convergence and non-zero-mode stability

The round S^4 has one conformal zero mode parametrising its overall scale. Write its radius as $a = e^{\sigma_0}\ell_\mathrm{P}$. With the convention $\Gamma = -\ln Z$ fixed in Sec. 4, the Euler piece contributes $+4a_\mathrm{SM}\sigma_0$ to the Euclidean effective action. On the selected damped contour the reduced exponent is therefore

$$f(\sigma_0) = Ce^{2\sigma_0} + 4a_\mathrm{SM}\sigma_0, \qquad C > 0, \tag{54}$$

and the weight is e^{-f}. Since

$$f'(\sigma_0) = 2Ce^{2\sigma_0} + 4a_\mathrm{SM} > 0, \tag{55}$$

Table 7: Detailed status of the ingredients entering Eq. (1).

Ingredient	Logical status	Established in
Compact-S^4 vacuum-energy ambiguity	renormalisation fact; absolute vacuum energy is not the compact observable	Sec. 3
Type-A datum a_{SM}	extraction theorem with free-scalar determinant sign audit	Thm. 1
Ordinary local anomaly backreaction	no-go result; gives an H^4 stress and no small linear branch	Prop. 2
Trace-free quotient projector	unique representative-independent local projection	Lemma 3
Primitive suppressed S^4 sector	selected decaying Lefschetz sector; opposite orientation falsifies the channel	Sec. 9
Boundary unit $u_b = 1$	exact reduced-Planck energy-density boundary defining the strict channel	Sec. 9
Paired-cap object	scalar matrix element; u_s is a thimble label and h an external source	Sec. 11
Source response	derived from the cap Euler response and the unique surviving local charge through four derivatives	Prop. 4
Proton endpoint	lightest stable QCD-generated colour-singlet trace-charge standard under the stated rule	Secs. 8 and 10
Matching hypothesis	endpoint conjugacy supplies the reflected interval; a reflection-even readout places the insertion on its fixed plane	Sec. 10
Matched scale	unique reflection fixed plane, conditional on the two-part matching hypothesis	Sec. 10
Finite determinants and common phases	source-independent factors cancel; source-dependent terms remain	Sec. 11
Compact global-source action	gravity-side physical postulate in the rigid dimensionless charge q_{WZ}	Sec. 12
Completed field equations	derived from the stated action-level normalisation	Thm. 6
Residual equation of state	$w = -1$ on a fixed global-source branch	Eq. (43)
Late-time amplitude	requires the regulated non-vacuum trace average to vanish	Eq. (46)

Table 8: Source and evaluation-point swap test. Entries are ratios to the strict paired-cap response.

Replacement	Response at h_*	q/q_{strict}
Einstein curvature charge, $\mathcal{C}_+/\mathcal{C}_{+,0} = x_h$	$\mathcal{A}_m r$	1
Overall source factor $c\mathcal{D}_+$	$c\mathcal{A}_m r$	c
Full-sphere logarithmic Weyl derivative	$\mathcal{A}_m$	r^{-1}
Cap-volume coordinate, $V/V_0 = x_h^2$	$\mathcal{A}_m r^2/2$	$r/2$
Selected source at $h = M_P$	$\mathcal{A}_m$	r^{-1}
Selected source at arithmetic mean	$\mathcal{A}_m/4 + O(r)$	$(4r)^{-1}$
Selected source at reflection plane	$\mathcal{A}_m r$	1
Selected source at $h = m_p$	$\mathcal{A}_m r^2$	r

Table 9: Per-field a-coefficients and Standard Model field-content sum. Each generation contains 15 Weyl fermions: three leptonic Weyl fields and 12 colour-counted quark Weyl fields.

Field	a	$720a$	SM multiplicity	contribution to $720a_{\mathrm{SM}}$
Real scalar	1/360	2	4	8
Weyl fermion	11/720	11	45	495
Vector boson	31/180	124	12	1488
Standard Model total				**1991**

the exponent has no real stationary point. The zero-mode calculation therefore diagnoses the boundary of the declared domain; it does not determine the Planck-curvature endpoint $u = 1$.

The strict sub-Planckian domain is $a \geq \ell_{\mathrm{P}}$, or $z = e^{2\sigma_0} \geq 1$. The damped integral is

$$I_{\mathrm{dom}}(C) = \frac{1}{2}\int_1^\infty z^{-2a_{\mathrm{SM}}-1}e^{-Cz}\,dz = \frac{1}{2}C^{2a_{\mathrm{SM}}}\Gamma(-2a_{\mathrm{SM}}, C), \qquad C > 0. \tag{56}$$

Its Lorentzian regulated form is

$$I_{L,\mathrm{dom}}(\epsilon) = \frac{1}{2}\int_1^\infty z^{-2a_{\mathrm{SM}}-1}e^{iCz-\epsilon z}\,dz = \frac{1}{2}(\epsilon - iC)^{2a_{\mathrm{SM}}}\Gamma(-2a_{\mathrm{SM}}, \epsilon - iC), \qquad \epsilon > 0. \tag{57}$$

The lower endpoint is finite because it is $z = 1$; the contour deformation controls the large-z end. Extending the integral to $z = 0$ gives the unbounded R1 reading and diverges for $a_{\mathrm{SM}} > 0$. Thus the Standard Model does not pass a separate “anomaly integrability” test: the physical domain does the endpoint regulation.

An unconditioned full-ray contour coefficient obtained by analytically continuing through $z = 0$ is not the marked-cap coefficient. It samples the excluded super-Planckian region, can carry a contour-dependent phase and magnitude, and neither multiplies q_{WZ} nor fixes its sign. The marked charge instead differentiates the sector-normalised conditional cap functional of Eq. (37), in which factors independent of the external compensator cancel before the response is taken.

At the Planck-curvature representative, the matter-anomaly correction to the classical action is measured by

$$\varepsilon = \left.\frac{a_{\mathrm{SM}}\kappa^2\Lambda}{24\pi^2}\right|_{\kappa^2\Lambda=1} \simeq 0.012. \tag{58}$$

The small value controls only this matter correction; it does not control the full quantum-gravitational expansion at Planck curvature. For nonconstant conformal modes, the anomaly-induced action contains the fourth-order Paneitz operator. In the convention used here its kinetic coefficient is proportional to a and has the stabilising sign for $a > 0$ [44, 66]. This is only a sign test; it does not prove that every metric and ghost mode is perturbatively controlled.

The zero-mode integral also clarifies the readings discussed in Sec. 14.2. Extending an unbounded modulus to $x = 0$ is divergent with the corrected determinant sign and enters the excluded super-Planckian domain. Restricting the integral to $x = M_{\mathrm{P}}^2/H^2 \geq 1$ produces the finite endpoint Laplace expansion e^{-B}/B and localises the response at the UV boundary. The R3 reading instead conditions on the primitive marked sector and applies the one-cap curvature-charge response to an external compensator on the fixed plane selected by the two-part matching hypothesis.

D Supporting details for the endpoint and scale selection

D.1 Saddle modulus versus external compensator

The round gravitational saddle family has a curvature modulus H_s and invariant measure dH_s/H_s. The strict primitive sector fixes this modulus at the Planck-boundary representative $u_s = 1$. The response variable h is different: it is the scale of the external Weyl compensator in the matter cap functional,

$$\widehat{g}_{\mu\nu}(h) = \frac{M_{\mathrm{P}}^2}{h^2} g_{s,\mu\nu}.$$

It is not integrated in the saddle measure. The compensator-induced transport U_h identifies the sourced boundary space $\mathcal{H}_{\Sigma,x_h\gamma_s}$ with the fixed fiducial space $\mathcal{H}_{\Sigma,\gamma_s}$, with its anomalous Jacobian retained in the matrix element. Together with Eq. (4), this makes $Z_{n,+}(h\,|\,u_s)$ a genuine two-argument scalar matrix element rather than one modulus assigned two values.

D.2 Why confinement defines a distinct infrared boundary

Above confinement, elementary thresholds are crossed by perturbative matching and decoupling. At confinement the appropriate degrees of freedom reorganise into colour singlets. The endpoint standard is required to be (i) a scheme-independent physical pole, (ii) a colour singlet, and (iii) stable in the full zero-temperature Standard Model. The proton is the lightest state satisfying all three [4] and, by Eq. (31), directly carries a normalised energy–momentum trace charge. Λ_{QCD} is scheme dependent; $2\pi T_c$ is a thermal crossover diagnostic [55]; pions and rho mesons are unstable; and a quoted 0^{++} glueball mass is a pure-Yang–Mills proxy [56]. The endpoint rule does not assert proton dominance of the vacuum trace spectral density.

D.3 Endpoint-conjugate reflection and the matched scale

With $s = \ln(h/m_p)$ and $L = \ln(M_{\mathrm{P}}/m_p)$, endpoint conjugacy identifies the two endpoint states as Osterwalder–Schrader conjugates. The induced endpoint-exchange reflection acts as $s \mapsto L - s$, equivalently

$$\mathcal{I}(h) = \frac{m_p M_{\mathrm{P}}}{h}.$$

The reflection-even local one-point coefficient lies on the unique fixed plane,

$$h_*^2 = m_p M_{\mathrm{P}}.$$

The same point also equalises the leading endpoint matching errors h^2/M_{P}^2 and m_p^2/h^2; this is a consistency check rather than an additional selection rule.

D.4 Boundary localisation of the compact saddle family

For the separate gravitational family $x_s = M_{\mathrm{P}}^2/H_s^2 \in [1,\infty)$ with $B(x_s) = 24\pi^2 x_s$, any polynomially bounded measure gives

$$\int_1^{\infty} p(x_s) e^{-Bx_s}\, dx_s = \frac{p(1)e^{-B}}{B}\left[1 + O(B^{-1})\right]. \tag{59}$$

This derives endpoint dominance inside the declared sub-Planckian domain. It does not turn the bounded integral into the marked cap coefficient: the former is R2, while the latter conditions on the primitive sector and differentiates an external matter source.

D.5 Alternative ultraviolet boundary conventions

The strict channel defines the gravitational validity boundary by the coupling appearing in the Einstein–Hilbert action, $u_b = \kappa^2\Lambda = 1$. Equivalently, $\Lambda = \bar{M}_{\rm P}^2$ and $V_\Lambda = \Lambda \bar{M}_{\rm P}^2 = \bar{M}_{\rm P}^4$. This gives $B = 24\pi^2$. Other order-one criteria define different channels: $G\Lambda = 1$ gives $B = 3\pi$, unit sphere radius in unreduced Planck lengths gives $B \simeq \pi$, and $\kappa^2\Lambda = 16\pi^2$ gives $B = 3/2$. They are not error bars on the strict channel. They show that observation sharply tests its exact Planck-boundary definition.

E Off-shell details of the dimensionless global-source action

The action used in the main text is

$$S_{\rm gs} = \int_M \left[\left(\frac{\mathcal{P}^2}{2}R - \mathcal{L}_m\right)\star 1 + \Lambda_b(F_4 - \star 1) - 8\pi(\mathcal{P}^2)^2 q_{\rm WZ}F_4\right]. \tag{60}$$

The independent rigid variables are $\mathcal{P}^2$, Λ_b, and the fixed dimensionless compact charge $q_{\rm WZ}$. No quantity proportional to $\mathcal{P}^2$ is introduced through a post-variation dictionary. Within its fixed cohomology class, $F_4 = dA_3$ is varied as a differential form independent of the metric; $F_4 = \star 1$ is imposed only after variation.

The variations give

$$\delta\Lambda_b : \quad F_4 = \star 1, \tag{61}$$

$$\delta A_3 : \quad d\big[\Lambda_b - 8\pi(\mathcal{P}^2)^2 q_{\rm WZ}\big] = 0, \tag{62}$$

$$\delta\mathcal{P}^2 : \quad \frac{1}{2}\int_M R\star 1 - 16\pi\mathcal{P}^2 q_{\rm WZ}\int_M F_4 = 0, \tag{63}$$

$$\delta g^{\mu\nu} : \quad \mathcal{P}^2 G_{\mu\nu} + \Lambda_b g_{\mu\nu} = T_{\mu\nu}. \tag{64}$$

Using $F_4 = \star 1$ gives

$$\langle R\rangle = 32\pi\mathcal{P}^2 q_{\rm WZ} = 4M_{\rm P}^2 q_{\rm WZ}.$$

The averaged metric trace then gives

$$\Lambda_b = 8\pi(\mathcal{P}^2)^2 q_{\rm WZ} + \frac{1}{4}\langle T\rangle,$$

and eliminating Λ_b gives Eq. (43).

The coefficient 8π is fixed by the convention already used for the observable, $q_{\rm WZ} \equiv G\Lambda$ with $G = (8\pi\mathcal{P}^2)^{-1}$. More generally, replacing 8π by α would give $\Lambda/M_{\rm P}^2 = (\alpha/8\pi)q_{\rm WZ}$ in vacuum. Thus the coefficient is not a post-variation ordering choice: it is the direct action-level implementation of the stated dimensionless source normalisation. The action itself remains the gravity-side postulate.

For the regulated Lorentzian late-time average, pressureless matter has $\rho_m \propto a^{-3}$ on an asymptotically de Sitter branch, so

$$\int^t a^3 T_m dt' \sim t, \qquad \int^t a^3 dt' \sim e^{3H_\infty t},$$

and their ratio vanishes. Radiation is trace-free, while a finite number of localised transitions grows more slowly than the de Sitter four-volume. This is the sufficient condition used in Eq. (46); it is not asserted for every recollapsing or finite-volume cosmology.

References

[1] A. G. Riess *et al.*, Observational evidence from supernovae for an accelerating universe and a cosmological constant, Astron. J. **116**, 1009–1038 (1998) [astro-ph/9805201].

[2] S. Perlmutter *et al.*, Measurements of Ω and Λ from 42 high-redshift supernovae, Astrophys. J. **517**, 565–586 (1999) [astro-ph/9812133].

[3] Planck Collaboration, Planck 2018 results. VI. Cosmological parameters, Astron. Astrophys. **641**, A6 (2020) [arXiv:1807.06209].

[4] F. Takahashi *et al.* (Particle Data Group), Review of Particle Physics, Int. J. Mod. Phys. A **41**, 2630011 (2026).

[5] S. Weinberg, The cosmological constant problem, Rev. Mod. Phys. **61**, 1 (1989).

[6] S. M. Carroll, The cosmological constant, Living Rev. Relativ. **4**, 1 (2001).

[7] J. Martin, Everything you always wanted to know about the cosmological constant problem (but were afraid to ask), Comptes Rendus Physique **13**, 566–665 (2012) [arXiv:1205.3365].

[8] C. P. Burgess, The cosmological constant problem: why it's hard to get dark energy from micro-physics, arXiv:1309.4133 [hep-th].

[9] S. Weinberg, Anthropic bound on the cosmological constant, Phys. Rev. Lett. **59**, 2607–2610 (1987).

[10] R. Bousso and J. Polchinski, Quantization of four-form fluxes and dynamical neutralization of the cosmological constant, JHEP **06**, 006 (2000).

[11] L. Susskind, The anthropic landscape of string theory, arXiv:hep-th/0302219.

[12] N. D. Birrell and P. C. W. Davies, *Quantum Fields in Curved Space*, Cambridge University Press, Cambridge (1982).

[13] L. S. Brown, Stress-tensor trace anomaly in a gravitational metric: scalar fields, Phys. Rev. D **15**, 1469–1483 (1977).

[14] J. S. Dowker and R. Critchley, Stress-tensor conformal anomaly for scalar, spinor, and vector fields, Phys. Rev. D **16**, 3390–3403 (1977).

[15] R. Ferrero, S. A. Franchino-Viñas, M. B. Fröb, and W. C. C. Lima, Universal definition of the nonconformal trace anomaly, Phys. Rev. Lett. **132**, 071601 (2024) [arXiv:2312.07666].

[16] R. M. Wald, *Quantum Field Theory in Curved Spacetime and Black Hole Thermodynamics*, University of Chicago Press, Chicago (1994).

[17] A. O. Barvinsky and G. A. Vilkovisky, The generalized Schwinger–DeWitt technique in gauge theories and quantum gravity, Phys. Rep. **119**, 1 (1985).

[18] E. Bianchi and C. Rovelli, Why all these prejudices against a constant?, arXiv:1002.3966 (2010).

[19] S. Hollands and R. M. Wald, Quantum field theory is not merely quantum mechanics applied to low energy effective degrees of freedom, Gen. Relativ. Gravit. **36**, 2595 (2004).

[20] M. J. Duff, Twenty years of the Weyl anomaly, Class. Quant. Grav. **11**, 1387 (1994).

[21] S. Deser and A. Schwimmer, Geometric classification of conformal anomalies in arbitrary dimensions, Phys. Lett. B **309**, 279 (1993).

[22] E. Baum, Zero cosmological constant from minimum action, Phys. Lett. B **133**, 185 (1983).

[23] S. W. Hawking, The cosmological constant is probably zero, Phys. Lett. B **134**, 403 (1984).

[24] S. Coleman, Why there is nothing rather than something: A theory of the cosmological constant, Nucl. Phys. B **310**, 643 (1988).

[25] R. Schützhold, Small cosmological constant from the QCD trace anomaly?, Phys. Rev. Lett. **89**, 081302 (2002).

[26] T. Padmanabhan, Cosmological constant: the weight of the vacuum, Phys. Rep. **380**, 235 (2003).

[27] T. Padmanabhan, The physical principle that determines the value of the cosmological constant, arXiv:1210.4174 [hep-th].

[28] H. Padmanabhan and T. Padmanabhan, CosMIn: The solution to the cosmological constant problem, Int. J. Mod. Phys. D **22**, 1342001 (2013) [arXiv:1302.3226].

[29] T. Padmanabhan and H. Padmanabhan, Cosmological constant from the emergent gravity perspective, Int. J. Mod. Phys. D **23**, 1430011 (2014) [arXiv:1404.2284].

[30] J. Solà, Cosmological constant and vacuum energy: old and new ideas, J. Phys. Conf. Ser. **453**, 012015 (2013) [arXiv:1306.1527].

[31] H. B. G. Casimir, On the attraction between two perfectly conducting plates, Proc. K. Ned. Akad. Wet. **51**, 793 (1948).

[32] R. L. Jaffe, Casimir effect and the quantum vacuum, Phys. Rev. D **72**, 021301 (2005).

[33] T. Jacobson, Thermodynamics of spacetime: the Einstein equation of state, Phys. Rev. Lett. **75**, 1260 (1995).

[34] S.-S. Chern, On the curvatura integra in a Riemannian manifold, Ann. Math. **46**, 674–684 (1945).

[35] A. L. Besse, *Einstein Manifolds*, Springer-Verlag, Berlin (1987).

[36] J. Wess and B. Zumino, Consequences of anomalous Ward identities, Phys. Lett. B **37**, 95 (1971).

[37] H. Osborn, Weyl consistency conditions and a local renormalisation group equation for general renormalisable field theories, Nucl. Phys. B **363**, 486–526 (1991).

[38] G. Aminov, C. Csáki, O. Telem, and S. Yankielowicz, Non-Abelian and type-A conformal anomalies from Euler descent, JHEP **07**, 053 (2026) [arXiv:2601.18892].

[39] M. Henneaux and C. Teitelboim, The cosmological constant and general covariance, Phys. Lett. B **222**, 195 (1989).

[40] N. Kaloper and A. Padilla, Sequestering the Standard Model vacuum energy, Phys. Rev. Lett. **112**, 091304 (2014).

[41] N. Kaloper, A. Padilla, D. Stefanyszyn, and G. Zahariade, Manifestly local theory of vacuum energy sequestering, Phys. Rev. Lett. **116**, 051302 (2016) [arXiv:1505.01492].

[42] J. Khoury, B. Muntz, and A. Padilla, A lapse in the cosmological constant problem, arXiv:2604.08659 [hep-th] (2026).

[43] R. J. Riegert, A non-local action for the trace anomaly, Phys. Lett. B **134**, 56 (1984).

[44] I. Antoniadis, P. O. Mazur, and E. Mottola, Physical states of the quantum conformal factor, Phys. Rev. D **55**, 4770 (1997) [hep-th/9509169]; see also I. Antoniadis, P. O. Mazur, and E. Mottola, Conformal invariance, dark energy, and CMB non-Gaussianity, J. Cosmol. Astropart. Phys. **09**, 024 (2012) [arXiv:1103.4164].

[45] Z. Komargodski and A. Schwimmer, On renormalization group flows in four dimensions, JHEP **12**, 099 (2011).

[46] S. M. Christensen and M. J. Duff, Quantizing gravity with a cosmological constant, Nucl. Phys. B **170**, 480 (1980).

[47] E. S. Fradkin and A. A. Tseytlin, Conformal anomaly in Weyl theory and anomaly free superconformal theories, Phys. Lett. B **134**, 187 (1984).

[48] D. Anninos, F. Denef, Y. T. A. Law, and Z. Sun, Quantum de Sitter horizon entropy from quasicanonical bulk, edge, sphere and topological string partition functions, JHEP **01**, 088 (2022) [arXiv:2009.12464].

[49] Y. T. A. Law, A compendium of sphere path integrals, JHEP **12**, 213 (2021) [arXiv:2012.06345].

[50] I. Jack and C. Poole, The a-function for gauge theories, JHEP **01**, 138 (2015) [arXiv:1411.1301].

[51] D. V. Vassilevich, Heat kernel expansion: user's manual, Phys. Rep. **388**, 279 (2003).

[52] T. Appelquist and J. Carazzone, Infrared singularities and massive fields, Phys. Rev. D **11**, 2856 (1975).

[53] D. J. Gross and F. Wilczek, Ultraviolet behavior of non-Abelian gauge theories, Phys. Rev. Lett. **30**, 1343 (1973).

[54] H. D. Politzer, Reliable perturbative results for strong interactions?, Phys. Rev. Lett. **30**, 1346 (1973).

[55] T. Bhattacharya *et al.* (HotQCD Collaboration), QCD phase transition with chiral quarks and physical quark masses, Phys. Rev. Lett. **113**, 082001 (2014) [arXiv:1402.5175].

[56] C. J. Morningstar and M. Peardon, The glueball spectrum from an anisotropic lattice study, Phys. Rev. D **60**, 034509 (1999) [hep-lat/9901004].

[57] X.-D. Ji, Breakup of hadron masses and energy-momentum tensor of QCD, Phys. Rev. D **52**, 271–281 (1995) [hep-ph/9502213].

[58] Y.-B. Yang, J. Liang, Y.-J. Bi, Y. Chen, T. Draper, K.-F. Liu, and Z. Liu, Proton mass decomposition from the QCD energy momentum tensor, Phys. Rev. Lett. **121**, 212001 (2018) [arXiv:1808.08677].

[59] G. W. Gibbons and S. W. Hawking, Action integrals and partition functions in quantum gravity, Phys. Rev. D **15**, 2752 (1977).

[60] G. W. Gibbons, S. W. Hawking, and M. J. Perry, Path integrals and the indefiniteness of the gravitational action, Nucl. Phys. B **138**, 141 (1978).

[61] J. Feldbrugge, J.-L. Lehners, and N. Turok, Lorentzian quantum cosmology, Phys. Rev. D **95**, 103508 (2017).

[62] J. Diaz Dorronsoro, J. J. Halliwell, J. B. Hartle, T. Hertog, and O. Janssen, Real no-boundary wave function in Lorentzian quantum cosmology, Phys. Rev. D **96**, 043505 (2017).

[63] DESI Collaboration, M. Abdul-Karim *et al.*, DESI DR2 results. II. Measurements of baryon acoustic oscillations and cosmological constraints, Phys. Rev. D **112**, 083515 (2025) [arXiv:2503.14738].

[64] DES Collaboration, T. M. C. Abbott *et al.*, Constraints on dynamical dark energy from multiple probes in the full Dark Energy Survey, arXiv:2605.27221 [astro-ph.CO].

[65] G. 't Hooft, Computation of the quantum effects due to a four-dimensional pseudoparticle, Phys. Rev. D **14**, 3432 (1976).

[66] P. O. Mazur and E. Mottola, The path integral measure, conformal factor problem and stability of the ground state of quantum gravity, Nucl. Phys. B **341**, 187 (1990).

[67] M. B. Fröb and J. Zahn, The Weyl anomaly in interacting quantum field theory on curved spacetimes, Ann. Henri Poincaré (2025), doi:10.1007/s00023-025-01635-2 [arXiv:2504.17854].

[68] R. Percacci, Unimodular quantum gravity and the cosmological constant, Found. Phys. **48**, 1364–1379 (2018) [arXiv:1712.09903].

[69] D. Buttazzo, G. Degrassi, P. P. Giardino, G. F. Giudice, F. Sala, A. Salvio and A. Strumia, Investigating the near-criticality of the Higgs boson, J. High Energy Phys. **12**, 089 (2013) [arXiv:1307.3536].

[70] G. Degrassi, S. Di Vita, J. Elias-Miró, J. R. Espinosa, G. F. Giudice, G. Isidori and A. Strumia, Higgs mass and vacuum stability in the Standard Model at NNLO, J. High Energy Phys. **08**, 098 (2012) [arXiv:1205.6497].

[71] E. Mottola, The effective theory of gravity and dynamical vacuum energy, J. High Energy Phys. **11**, 037 (2022) [arXiv:2205.04703].

[72] J.-L. Lehners, Review of the no-boundary wave function, Phys. Rep. **1022**, 1 (2023) [arXiv:2303.08802].

[73] D. M. Capper and M. J. Duff, Trace anomalies in dimensional regularization, Nuovo Cimento A **23**, 173 (1974).

[74] J. L. Cardy, Is there a c-theorem in four dimensions?, Phys. Lett. B **215**, 749 (1988).

[75] J. B. Hartle and S. W. Hawking, Wave function of the universe, Phys. Rev. D **28**, 2960 (1983).

[76] A. Vilenkin, Quantum creation of universes, Phys. Rev. D **30**, 509(R) (1984).

[77] E. Witten, Analytic continuation of Chern–Simons theory, AMS/IP Stud. Adv. Math. **50**, 347 (2011) [arXiv:1001.2933].

[78] N. Blinov and P. Draper, Densities of states and the CKN bound, arXiv:2107.03530 [hep-ph].

[79] B. L. Giacchini, T. de Paula Netto, and I. L. Shapiro, Effective quantum gravity, cosmological constant and the Standard Model of particle physics, Phys. Rev. D **105**, 126025 (2022) [arXiv:2112.06314].

[80] S. J. Brodsky, A. Deur, and C. D. Roberts, Artificial dynamical effects in quantum field theory, Nature Rev. Phys. **4**, 489–495 (2022) [arXiv:2202.06051].

[81] T. Jacobson and M. R. Visser, Partition function for a volume of space, Phys. Rev. Lett. **130**, 221501 (2023) [arXiv:2212.10607].

[82] C. Corianò, M. Cretì, and M. M. Maglio, Broken scale invariance and the regularization of a conformal sector in gravity with Wess–Zumino actions, Phys. Lett. B **843**, 138003 (2023) [arXiv:2301.07460].

[83] P. Jiroušek, Unimodular approaches to the cosmological constant problem, Universe **9**, 131 (2023) [arXiv:2301.01662].

[84] B. S. Kay, Quantum field theory in curved spacetime (2nd edition), arXiv:2308.14517 [gr-qc].

[85] R. Larue, J. Quevillon, and R. Zwicky, Trace anomaly of Weyl fermions via the path integral, JHEP **12**, 064 (2023) [arXiv:2309.08670].

[86] G. Hiller, T. Höhne, D. F. Litim, and T. Steudtner, Vacuum stability in the Standard Model and beyond, Phys. Rev. D **110**, 115017 (2024) [arXiv:2401.08811].

[87] J. Maldacena, Real observers solving imaginary problems, arXiv:2412.14014 [hep-th].

[88] B. Wang, F. He, G. Wang, T. Draper, J. Liang, K.-F. Liu, and Y.-B. Yang, Trace anomaly form factors from lattice QCD, Phys. Rev. D **109**, 094504 (2024) [arXiv:2401.05496].

[89] Y. Chen, D. Stanford, H. Tang, and Z. Yang, On the phase of the de Sitter density of states, JHEP **05**, 068 (2026) [arXiv:2511.01400].

[90] K. Tanaka, Proton mass decompositions in the NNLO QCD, arXiv:2511.18310 [hep-ph].

[91] D. Bollweg, H.-T. Ding, X. Gao, R. Luo, and S. Mukherjee, Lattice-QCD validation of hadron mass and trace-anomaly decomposition sum rules, Phys. Rev. Lett., accepted (2026), doi:10.1103/5n46-717z [arXiv:2601.13070].

[92] S. Giombi and Z. Sun, The phase of de Sitter higher spin gravity, arXiv:2601.15257 [hep-th].

[93] A. Perez and D. Sudarsky, Renormalization of the quantum stress tensor fluctuations and the limits of semiclassical gravity, arXiv:2512.17789 [gr-qc].

[94] S. Giombi and I. R. Klebanov, Interpolating between a and F, JHEP **03**, 117 (2015) [arXiv:1409.1937].

[95] H. Elvang and T. M. Olson, RG flows in d dimensions, the dilaton effective action, and the a-theorem, JHEP **03**, 034 (2013) [arXiv:1209.3424].

[96] D. V. Fursaev, Conformal anomalies of CFTs with boundaries, JHEP **12**, 112 (2015) [arXiv:1510.01427].

[97] C. P. Herzog, K.-W. Huang, and K. Jensen, Universal entanglement and boundary geometry in conformal field theory, JHEP **01**, 162 (2016) [arXiv:1510.00021].

[98] A. Jaffe and G. Ritter, Reflection positivity and monotonicity, J. Math. Phys. **49**, 052301 (2008) [arXiv:0705.0712].

[99] K.-H. Neeb and G. Ólafsson, Reflection positivity and conformal symmetry, J. Funct. Anal. **266**, 2174–2224 (2014) [arXiv:1206.2039].

[100] H. Casini, M. Huerta, and R. C. Myers, Towards a derivation of holographic entanglement entropy, JHEP **05**, 036 (2011) [arXiv:1102.0440].